

## Supporting Information

# ***In vitro* characterization and stability profiles of antibody-fluorophore conjugates generated through cross-linking or lysine bioconjugation.**

Camille Martin <sup>1</sup>, Guillaume Brachet <sup>2,3</sup>, Cyril Colas <sup>4,5</sup>, Emilie Allard-Vannier <sup>6</sup>, Claire Kizlik-Masson <sup>3</sup>, Clara Esnault <sup>1</sup>, Renaud Respaud <sup>7</sup>, Caroline Denevault-Sabourin <sup>1</sup>, Igor Chourpa <sup>6</sup>, Valérie Gouilleux-Gruart <sup>2,3</sup>, Marie-Claude Viaud-Massuard <sup>1</sup>, and Nicolas Joubert <sup>1,\*</sup>

<sup>1</sup> GICC EA7501, Equipe IMT, Université de Tours, UFR des Sciences Pharmaceutiques, 31 Avenue Monge, 37200 Tours, France.

<sup>2</sup> Laboratoire d'immunologie, CHRU Tours, 10 Bd Tonnelé, 37000 Tours, France.

<sup>3</sup> GICC EA7501, Equipe FRAME, Université de Tours, 10 Bd Tonnelé, 37000 Tours, France.

<sup>4</sup> ICOA UMR 7311 CNRS, Université d'Orléans, Pôle de Chimie, Rue de Chartres, BP 6759, 45067 Orléans Cedex 2, France.

<sup>5</sup> CBM, UPR4301 CNRS, Rue Charles Sadron, 45071 Orléans, France.

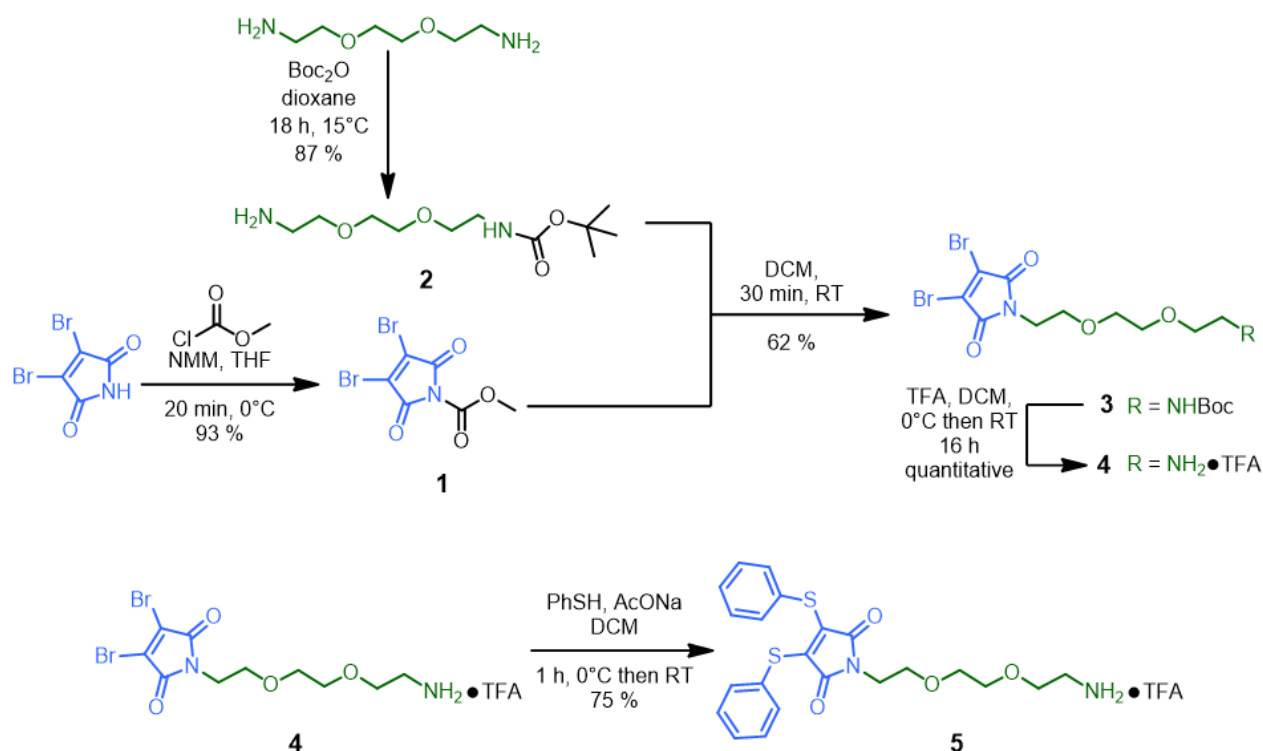
<sup>6</sup> NMNS EA 6295, 31 Avenue Monge, 37200 Tours, France.

<sup>7</sup> INSERM U1100, Université de Tours, 10 Bd Tonnelé, 37000 Tours, France.

\* Correspondence: nicolas.joubert@univ-tours.fr

### **Table of content**

Synthesis of compounds <b>1</b> , <b>2</b> , <b>3</b> , <b>4</b> and <b>5</b> .....	S2
NMR spectra of new compounds .....	S4
Optimized equivalents for lysine conjugation .....	S12
Deconvoluted spectra of AFCs and native mAbs .....	S12
Molecular weights of AFCs expected and observed by MS.....	S14
Raw mass spectra of native and deglycosylated mAbs, AFCs and associated TIC.....	S15
HER2 binding of AFCs TTZ-SGM-FLU <b>7b</b> and TTZ-FLU <b>9b</b> .....	S28
CD20 binding of AFCs RTX-SGM-FLU <b>8b</b> , RTX-FLU <b>10b</b> at pH7 and pH6, n = 3.....	S28
Statistical analysis on CD20 binding.....	S29
Models representing paratopes of rituximab and trastuzumab .....	S29
UV-visible absorption of AFCs .....	S30
Stability of AFCs upon storage.....	S31
Stability of AFCs to pH variation .....	S32



**Scheme S1.** Synthesis of compounds **1**, **2**, **3**, **4** and **5**

### 2,3-Dibromo-N-methoxycarbonylmaleimide **1**

2,3-Dibromomaleimide (2.82 g, 11.065 mmol) was dissolved in dry tetrahydrofuran (99 mL) and cooled down to  $0^\circ\text{C}$ . *N*-Methylmorpholine (1.220 mL, 11.065 mmol) and methylchloroformate (854  $\mu\text{L}$ , 11.065 mmol) were added and stirred at  $0^\circ\text{C}$  for 20 min under inert atmosphere. Dichloromethane was added (120 mL) and the organic phase was washed with water ( $3 \times 40$  mL), dried over magnesium sulphate ( $\text{MgSO}_4$ ) and concentrated under reduced pressure to give **1** as a purple solid (3.21 g, 93%).  $^1\text{H NMR}$  (300 MHz,  $\text{CDCl}_3$ )  $\delta$  (ppm) 4.00 (s, 3H,  $\text{CH}_3$ ).  $^{13}\text{C NMR}$  (75 MHz,  $\text{CDCl}_3$ )  $\delta$  (ppm) 159.3 ( $\times 2$ ), 147.0, 131.5 ( $\times 2$ ), 54.8.<sup>1</sup>

### 1-(*t*-Butyloxycarbonyl-amino)-3,6-dioxa-8-octaneamine **2**

1,8-Diamino-3,6-dioxaoctane (1.058 mL, 7.254 mmol) was dissolved in dioxane (4 mL) and cooled down to  $10$ - $15^\circ\text{C}$ , di-*t*-butyl pyrocarbonate (264 mg, 1.209 mmol) in dioxane (4 mL) was added slowly at  $10$ - $15^\circ\text{C}$  and stirred at  $15^\circ\text{C}$  overnight. Dioxane was removed under reduced pressure and water was added. The aqueous residue was extracted with ethyl acetate ( $5 \times 50$  mL), combined organic phases were washed with brine ( $5 \times 50$  mL), dried over  $\text{MgSO}_4$  and concentrated under reduced pressure to give **2** (261 mg, 87%) as a colourless oil.  $^1\text{H NMR}$  (300 MHz,  $\text{CDCl}_3$ )  $\delta$  (ppm) 5.18 (broad s, 1H,  $\text{NH}(\text{CO})$ ), 3.62-3.53 (m, 8H,  $\text{CH}_2\text{-O}$ ), 3.53-3.31 (m, 2H,  $\text{CH}_2\text{-N}$ ), 2.90 (t,  $J = 4.9$  Hz, 2H,  $\text{CH}_2\text{-NH}(\text{CO})$ ), 1.44 (s, 9H,  $\text{CH}_3$ ).<sup>2</sup>

### 3,4-Dibromomaleimide-N-8-(*t*-Butyloxycarbonyl-amino)-3,6-dioxa-octane **3**

**1** (500 mg, 1.028 mmol) was dissolved in dry dichloromethane (6.6 mL), a solution of freshly prepared **2** (397 mg, 1.028 mmol) in dry dichloromethane (6.6 mL) was added and it was stirred under argon at room temperature for 30 min. Water was added and the organic phase was

washed with water (3×15 mL), dried MgSO<sub>4</sub> and solvent was removed by evaporation. The crude mixture was purified by flash chromatography (SiO<sub>2</sub>, dichloromethane/methanol 99:1) to give **3** (485 mg, 62%) as a pale beige solid. <sup>1</sup>H NMR (300 MHz, CDCl<sub>3</sub>) δ (ppm) 4.98 (broad s, 1H, NH(CO)), 3.83 (t, *J* = 5.4 Hz, 2H CH<sub>2</sub>), 3.67 (t, *J* = 5.4 Hz, 2H, CH<sub>2</sub>-O), 3.62-3.58 (m, 2H, CH<sub>2</sub>-O), 3.58-3.53 (m, 2H, CH<sub>2</sub>-O), 3.50 (t, *J* = 5.1 Hz, 2H, CH<sub>2</sub>-O), 3.33-3.26 (m, 2H, CH<sub>2</sub>-NH(CO)), 1.44 (s, 9H, CH<sub>3</sub>). <sup>13</sup>C NMR (75 MHz, CDCl<sub>3</sub>) δ (ppm) 163.9 (×2), 156.0, 129.5 (×2), 77.2, 70.3, 70.2, 70.0, 67.6, 38.8 (×2), 28.4 (×3). HRAM (ESI): *m/z* calc.= 484.9917, found 484.9911.

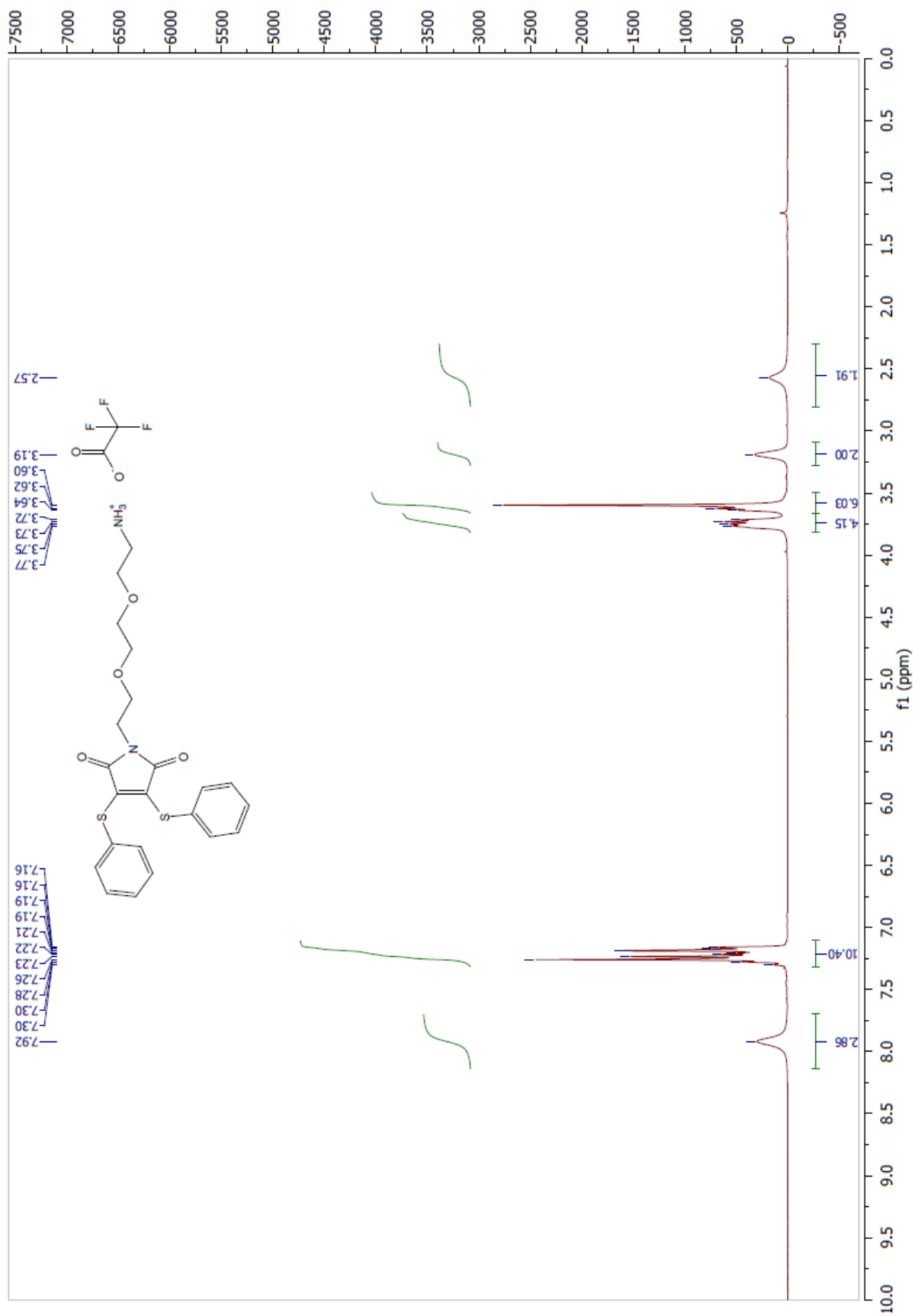
#### *3,4-Dibromomaleimide-N-8-amino-3,6-dioxaoctane 4*

**3** (284 mg, 0.584 mmol) was dissolved in dry dichloromethane (CH<sub>2</sub>Cl<sub>2</sub>) (6.3 mL) and cooled down to 0 °C. Trifluoroacetic acid (TFA) (626 μL, 10% solution in CH<sub>2</sub>Cl<sub>2</sub>) was added at 0 °C and it was stirred at room temperature (rt) overnight. The crude was concentrated under reduced pressure and TFA was co-evaporated with CH<sub>2</sub>Cl<sub>2</sub> (3×30 mL) to give the trifluoroacetic salt of **4** (295 mg, 100%) as a white solid. <sup>1</sup>H NMR (300 MHz, CDCl<sub>3</sub>) δ (ppm) 7.74 (broad s, 3H, NH<sub>3</sub>), 3.83 (t, *J* = 9.9 Hz, 2H, CH<sub>2</sub>), 3.74 (t, *J* = 9.7 Hz, 2H, CH<sub>2</sub>-O), 3.67-3.58 (m, 6H, CH<sub>2</sub>-O), 3.30-3.21 (m, 2H, CH<sub>2</sub>-N). <sup>13</sup>C NMR (75 MHz, CDCl<sub>3</sub>) δ (ppm) 164.5 (×2), 159.9, 129.7 (×2), 77.4, 70.1, 69.9, 68.3, 66.3, 40.2, 39.2. HRAM (ESI): *m/z* calc.= 384.9393, found 384.9392.

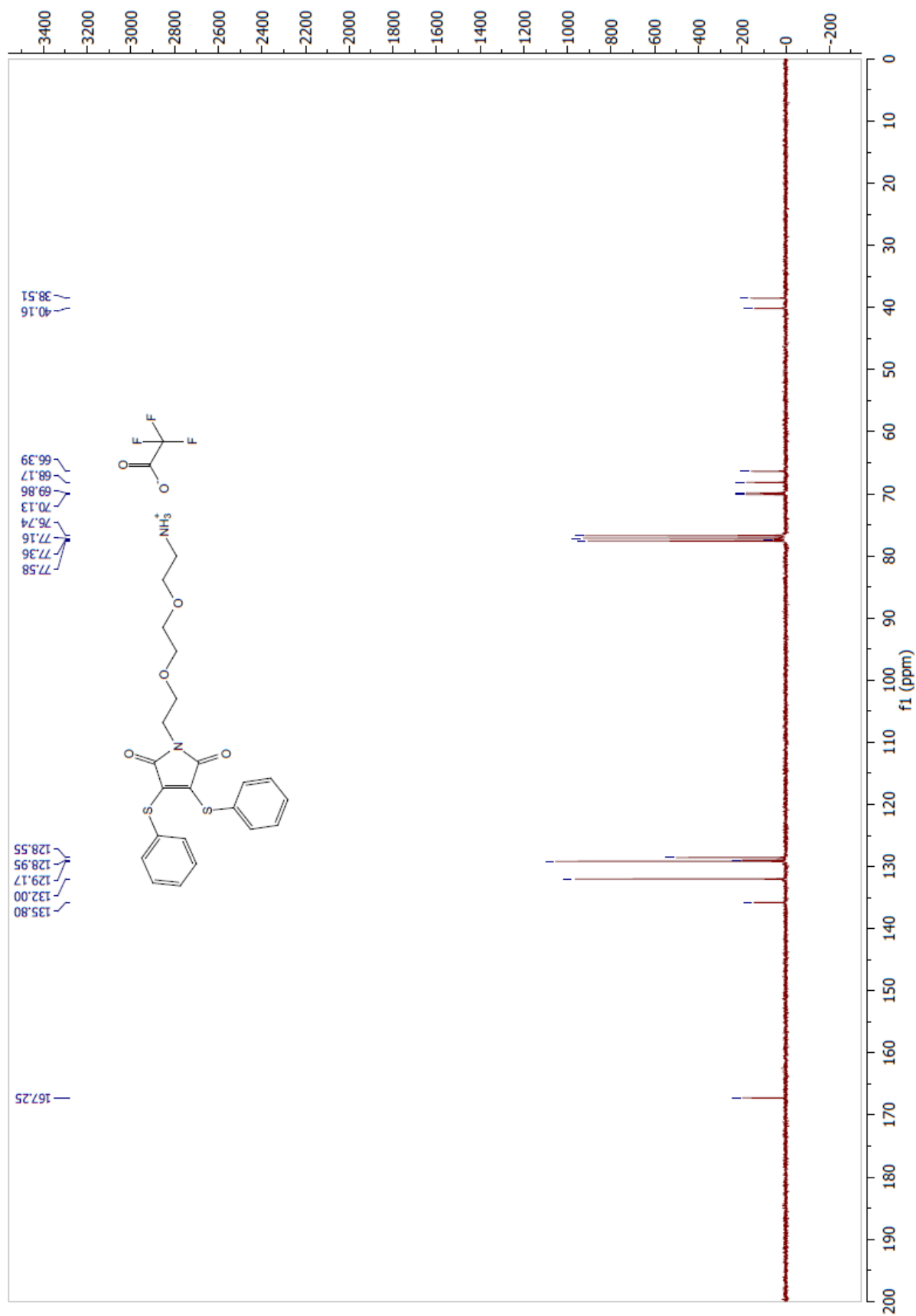
#### *3,4-Dithiophenylmaleimide-N-8-amino-3,6-dioxaoctane 5*

A solution of the trifluoroacetic salt of **4** (52 mg, 0.103 mmol) in dry CH<sub>2</sub>Cl<sub>2</sub> (1 mL) was added dropwise to an ice-cold stirring solution of sodium acetate (27 mg, 0.309 mmol) and thiophenol (31 μL, 0.297 mmol) in dry CH<sub>2</sub>Cl<sub>2</sub> (1 mL). The solution turned yellow and was stirred at rt for 1 h. It was cooled down to 0 °C and treated with HCl 1N dropwise. After CH<sub>2</sub>Cl<sub>2</sub> extractions (3×10 mL), organic phases were combined, dried over MgSO<sub>4</sub> and concentrated under reduced pressure to give an orange oil. It was taken up in a minimum amount of CH<sub>2</sub>Cl<sub>2</sub> and put on a cake of silica. It was washed with cyclohexane to remove the excess of thiophenol and then used as a solid deposit for purification by flash chromatography (SiO<sub>2</sub>, CH<sub>2</sub>Cl<sub>2</sub>/MeOH 97:3) to give the trifluoroacetic salt of **5** (43 mg, 75%) as an orange oil. <sup>1</sup>H NMR (300 MHz, CDCl<sub>3</sub>) δ (ppm) 8.12 (s broad, 3H, NH<sub>3</sub>), 7.26-7.16 (m, 10H, Ph), 3.80-3.48 (m, 10H, CH<sub>2</sub>, CH<sub>2</sub>-O), 3.20-3.09 (m, 2H, CH<sub>2</sub>-N). <sup>13</sup>C NMR (75 MHz, CDCl<sub>3</sub>) δ 167.3 (×2), 135.8, 132.0 (×4), 129.2 (×4), 129.0 (×4), 128.6 (×2), 77.4, 70.1, 69.9, 68.2, 66.4, 40.2, 38.5. <sup>19</sup>F (282 MHz, CDCl<sub>3</sub>) δ (ppm) -75. HRAM (ESI): *m/z* calc.= 445.1250, found 445.1250.

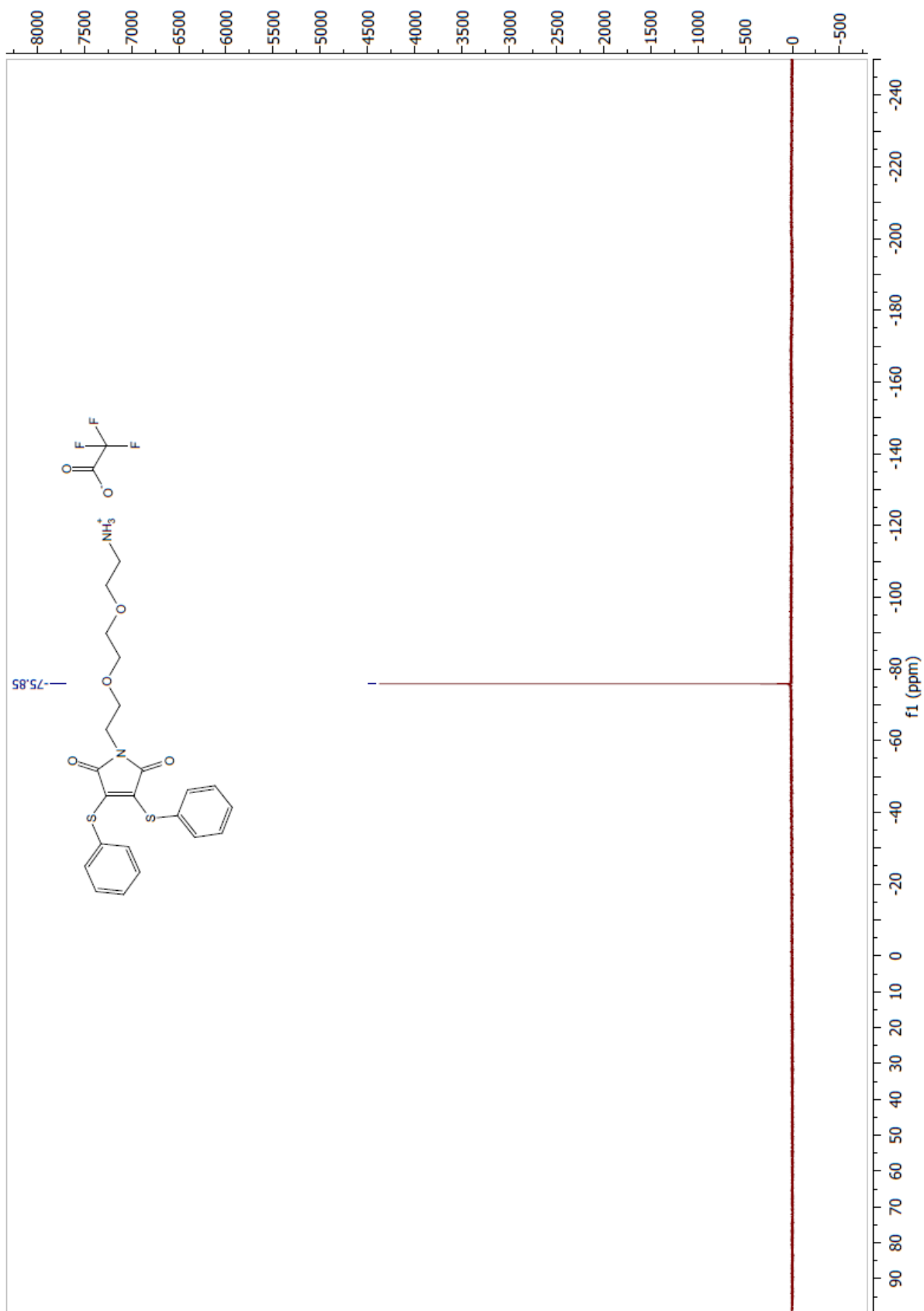
Compound 5 – <sup>1</sup>H NMR



Compound 5 – <sup>13</sup>C NMR

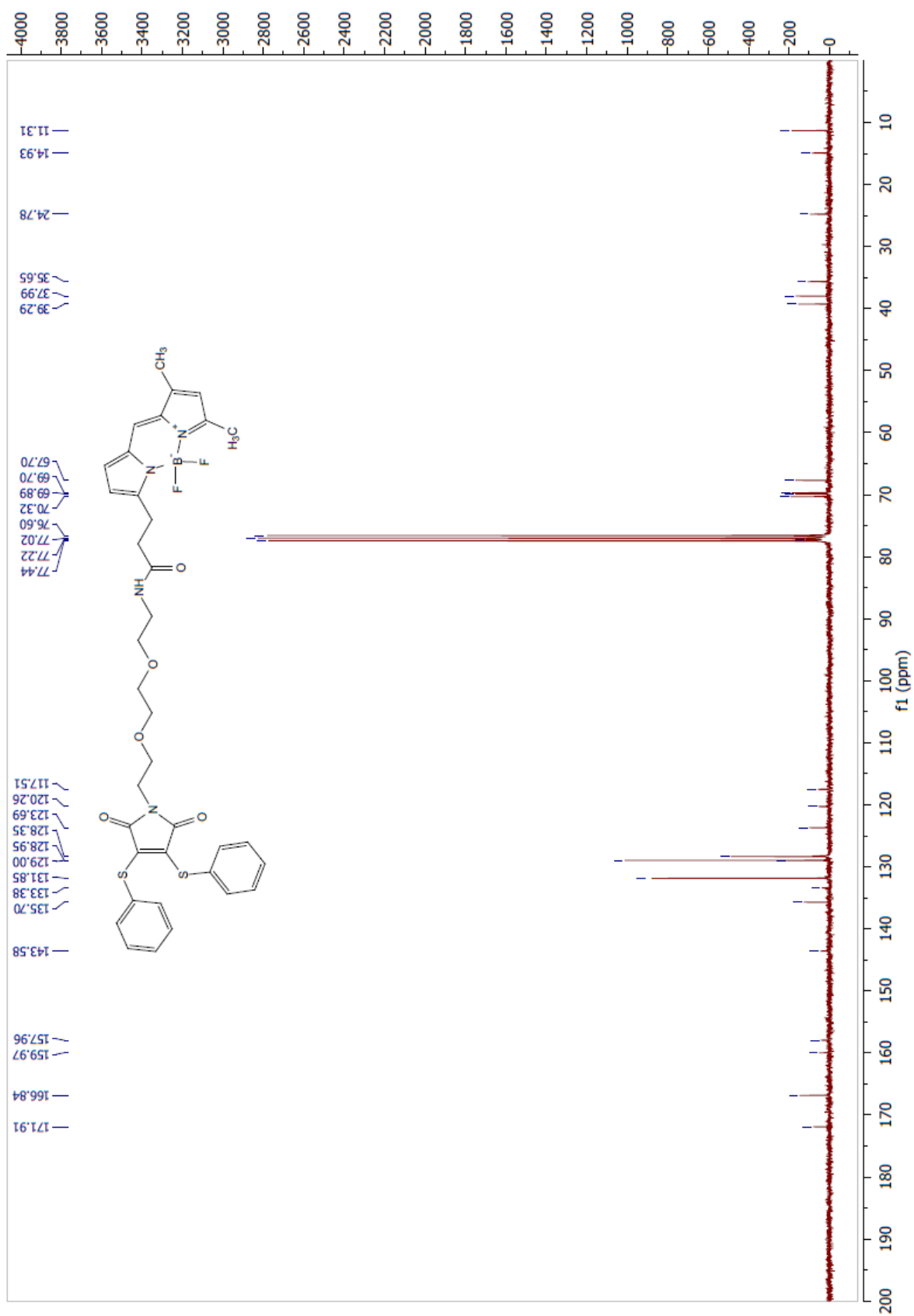


Compound 5 – <sup>19</sup>F NMR

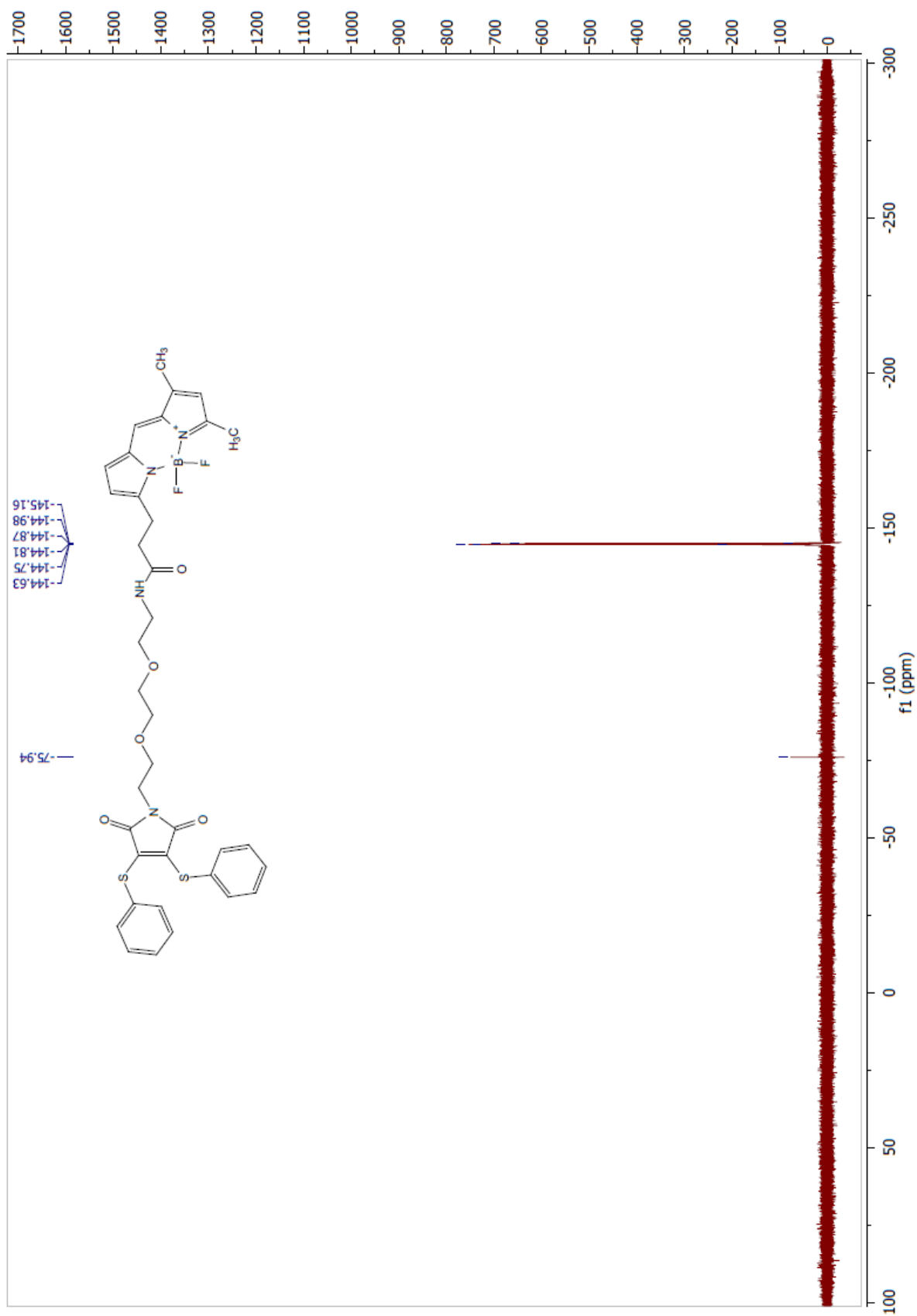




Compound 6a – <sup>13</sup>C NMR



Compound 6a – 19F NMR





Compound 6b – <sup>13</sup>C NMR

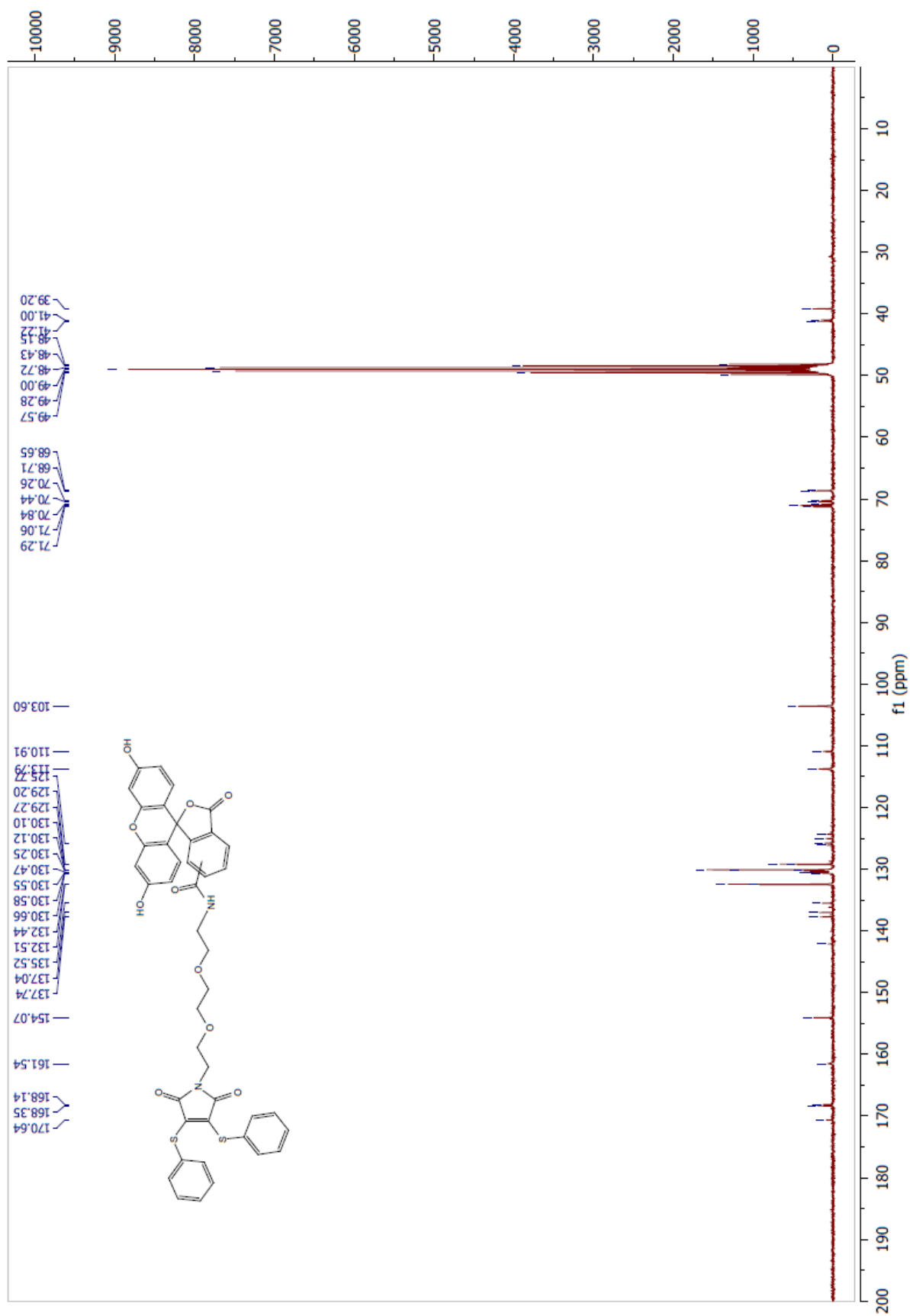


**Table S1.** Optimized equivalents for lysine conjugation

mAb	Fluorophore	eq	Volume of 0.01M ( $\mu$ L)
TTZ	BDP	3.3	4.0
TTZ	FLU	10	12
RTX	BDP	2.7	3.2
RTX	FLU	10	12

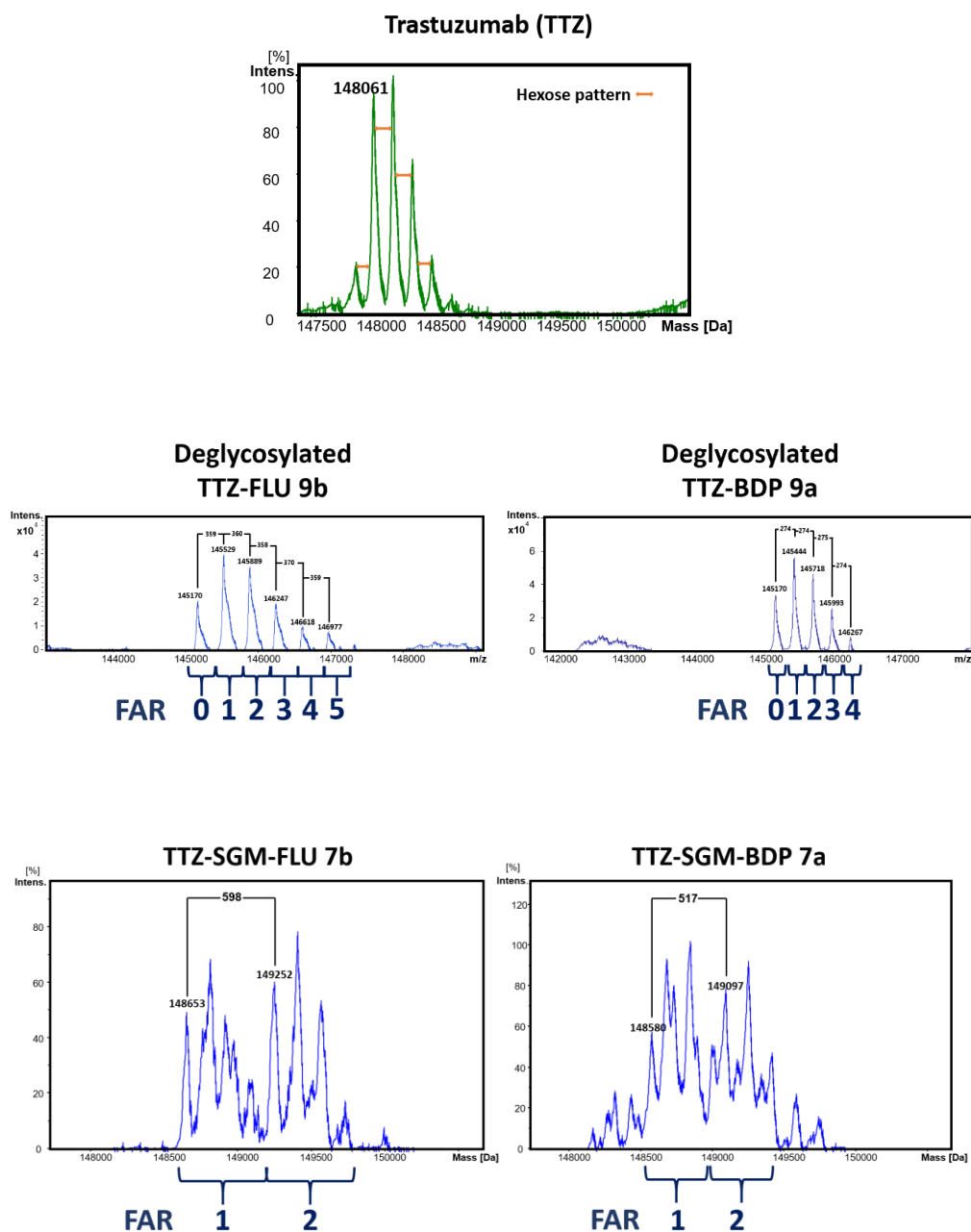


**Figure S1.** Deconvoluted spectra of AFCs and native trastuzumab. Deglycosylation was performed using PNGase F on lysines samples diluted to 1 mg/mL. Samples were incubated 6 h at 37 °C prior to MS analysis.

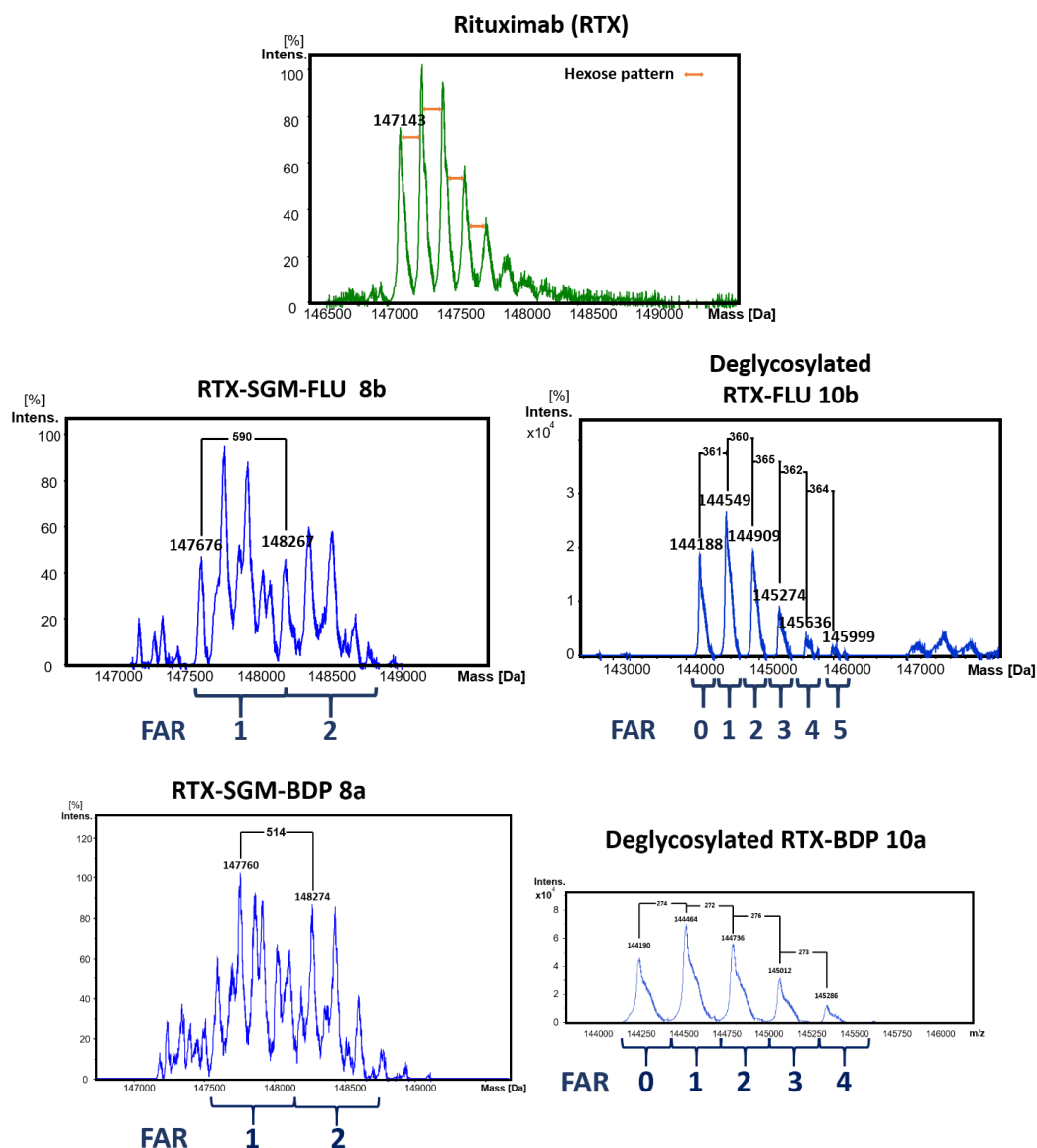


**Figure S2.** Deconvoluted spectra of AFCs and native rituximab. Deglycosylation was performed using PNGase F on lysines samples diluted to 1 mg/mL. Samples were incubated 6 h at 37 °C prior to MS analysis.

Mass spectrometry analysis was used to determine FAR distribution of all AFCs. We used an electrospray ionisation (ESI) source, producing multi-charged ions. Classical glycosylation profiles of native antibodies were observed. For labelled mAbs, average FAR was calculated from signal integration of deconvoluted mass spectra, either on glycosylated or deglycosylated proteins. The small mass increment resulting for lysine conjugation required deglycosylation before analysis to avoid signal overlap between glycosylation and conjugation and to identify each FAR species unambiguously. While mass increment resulting from cross-linking was higher and sufficiently important to allow discrepancies between different FAR species. This is why, for cross-linking labelling technology, we chose to analyse the unmodified glycosylated AFC, while we deglycosylated the AFCs resulting from lysine labelling.

Second generation maleimide (SGM) are heterocycle known in the antibody-drug conjugate (ADC) field of research. For bioconjugation using SGM (dithiophenylmaleimide or dibromomaleimide) you can see the published work of our group (*Org. Biomol. Chem.*, **2018**, *16*, 1882–1889; *Bioconjugate Chem.* **2018**, *29*, 3516–3521; patent WO2015004400), from Jackson *et al.* (Igenica; *Mol. Pharmaceuticals* **2015**, *12*, 3986–3998) or from Baker *et al.* (UCL; *Org. Biomol. Chem.*, **2014**, *12*, 7261–7269, etc).

Classical glycosylation profiles of native antibodies were observed. For labelled mAbs, average FAR was calculated from signal integration of deconvoluted mass spectra, either on glycosylated or deglycosylated proteins. The small mass increment resulting for lysine conjugation required deglycosylation before analysis to identify each FAR species. While mass increment resulting from cross-linking was higher and sufficiently important to allow discrepancies between different FAR species. This is why, for cross-linking labelling technology, we chose to analyze the unmodified glycosylated AFC, while we deglycosylated the AFCs resulting from lysine labelling. SGM is able to cross-link previously reduced disulfide bridges, as demonstrated in these several papers. Experimentally, it is very simple to verify: for example for the linker **6a** (BODIPY-SGM), the mass increment when conjugated on antibody is 520 Da per dye conjugated, which correspond to the mass of the linker minus two SPh moieties (2 x 109). One SPh is removed from the linker only after bioconjugation of a sulfhydryl from a cysteine. Therefore losing two SPh means that the linker is fixed on two cysteine residues (see TTZ-SGM-BDP **7a** in Figure S2 for an example). The average FAR (or DAR) calculation method has been validated in our previous papers (quoted above).

**Table S2** and **Table S3**. Molecular weights of AFCs expected and observed by MS

AFC	MW FAR0		MW FAR1		MW FAR2		MW FAR3		MW FAR4		MW FAR5	
	Exp.	Obs.										
TTZ-BDP <b>9a</b>	145170	145170	145444	145444	145718	145718	145992	145993	146266	146267	146540	-
TTZ-FLU <b>9b</b>	145170	145170	145525	145529	145880	145889	146235	146247	146590	146618	146945	146977
RTX-BDP <b>10a</b>	144187	144190	144461	144464	144735	144736	145009	145012	145283	145286	145557	-
RTX-FLU <b>10b</b>	144187	144188	144542	144549	144897	144909	145252	145274	145607	145636	145962	145999

AFC	MW FAR1		MW FAR2	
	Exp.	Obs.	Exp.	Obs.
TTZ-SGM-BDP <b>7a</b>	148650	148653	149240	149252
TTZ-SGM-FLU <b>7b</b>	148575	148580	149090	149097
RTX-SGM-BDP <b>8a</b>	147732	147676	148322	148267
RTX-SGM-FLU <b>8b</b>	147657	147660	148172	148274

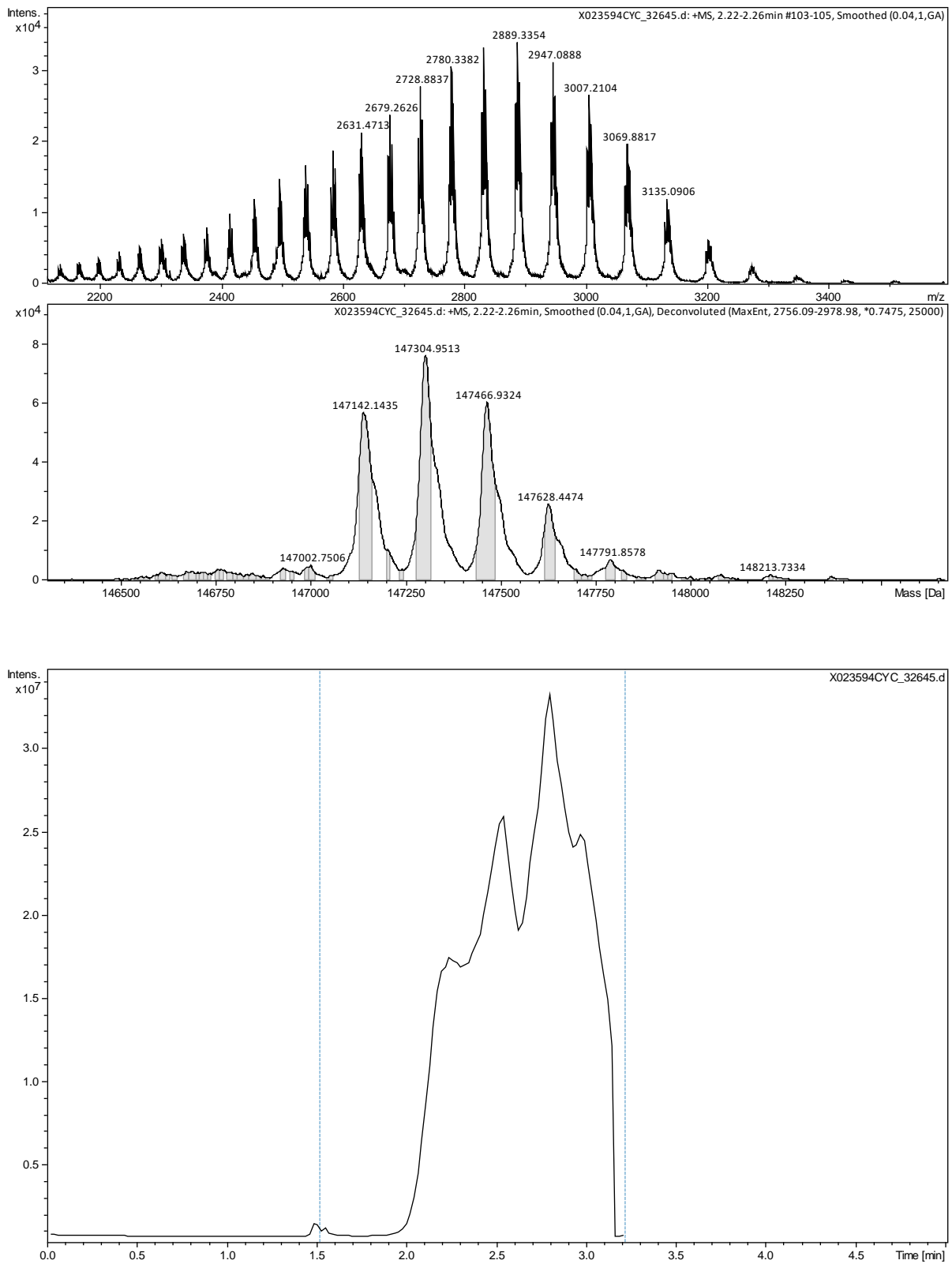
To assess the fluorophore-to-antibody ratio (FAR), we looked at the mass increase between the different species in solution and compared expected (Exp.) and observed (Obs.) masses. Arbitrarily, for samples **7** and **8**, we chose to focus on the first intense glycosylation of antibodies as the value for FAR0.

**Table 1**. AFCs obtained from disulfide cross-linking or lysine bioconjugation technologies onto trastuzumab or rituximab with BODIPY or fluorescein dyes.

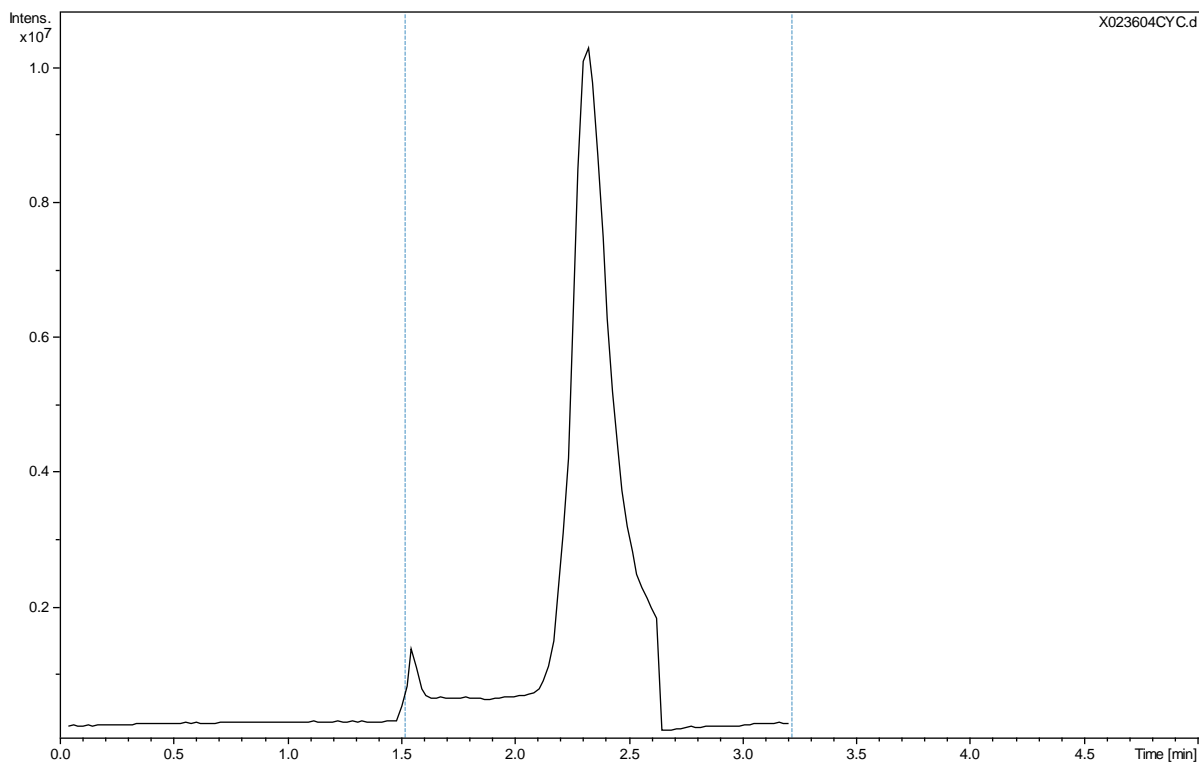
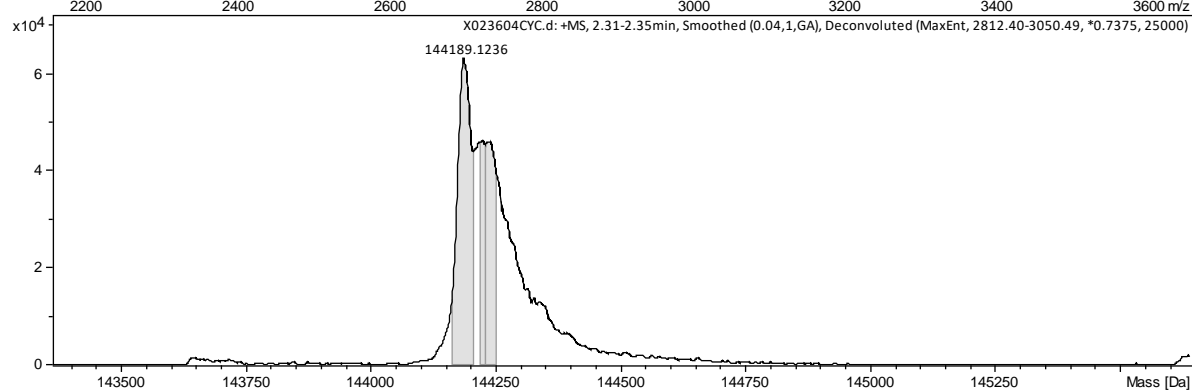
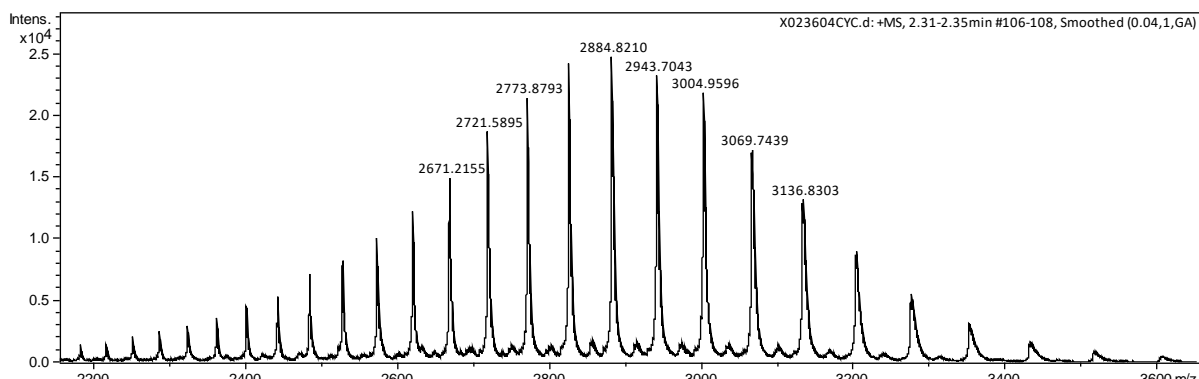
Antibody	Compound used for bioconjugation	AFC
Trastuzumab	BODIPY-SGM <b>6a</b>	TTZ-SGM-BDP <b>7a</b>
Trastuzumab	Fluorescein-SGM <b>6b</b>	TTZ-SGM-FLU <b>7b</b>
Rituximab	BODIPY-SGM <b>6a</b>	RTX-SGM-BDP <b>8a</b>
Rituximab	Fluorescein-SGM <b>6b</b>	RTX-SGM-FLU <b>8b</b>
Trastuzumab	BODIPY-NHS	TTZ-BDP <b>9a</b>
Trastuzumab	Fluorescein-NHS	TTZ-FLU <b>9b</b>
Rituximab	BODIPY-NHS	RTX-BDP <b>10a</b>
Rituximab	Fluorescein-NHS	RTX-FLU <b>10b</b>

**Figure S3.** Raw mass spectra of native and deglycosylated mAbs, AFCs and associated TIC

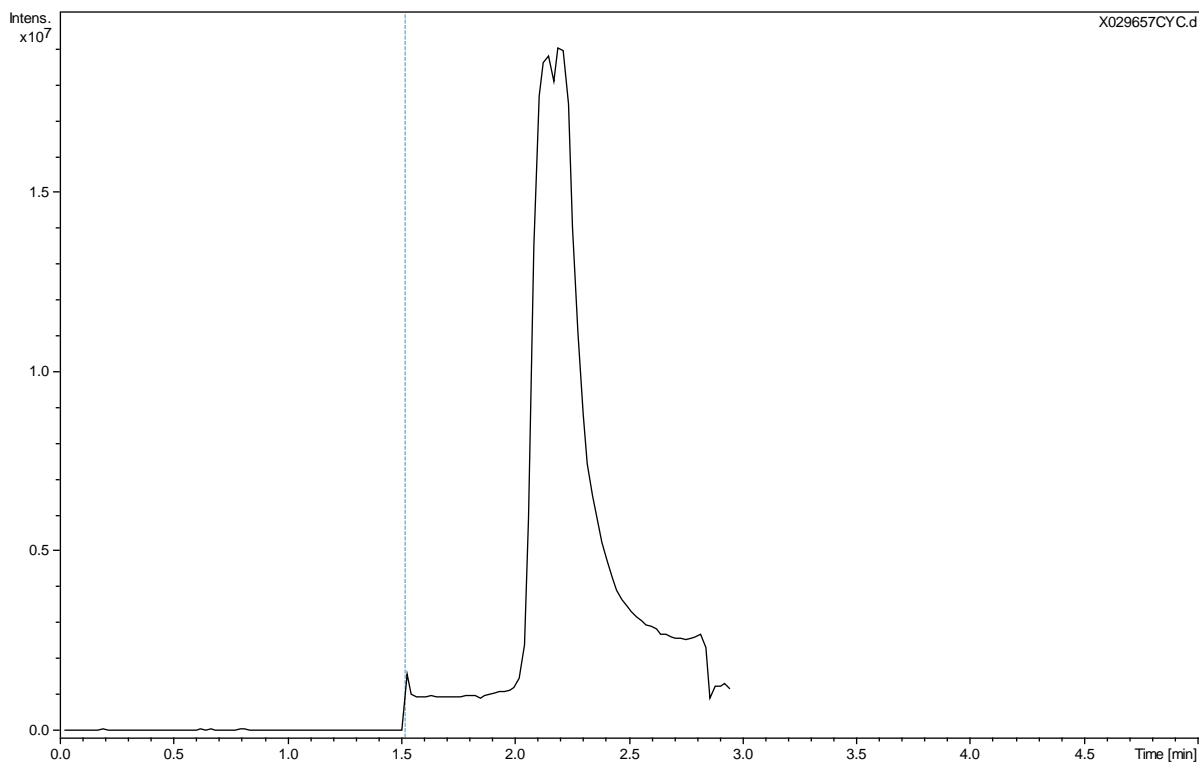
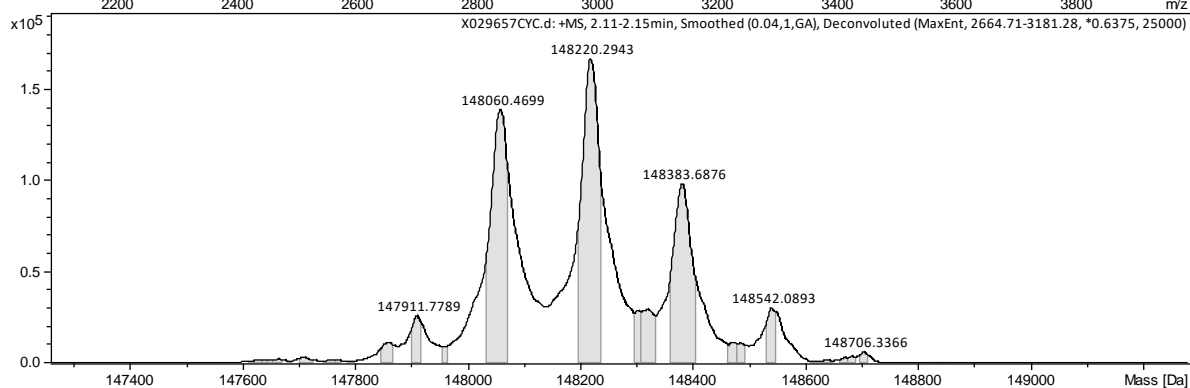
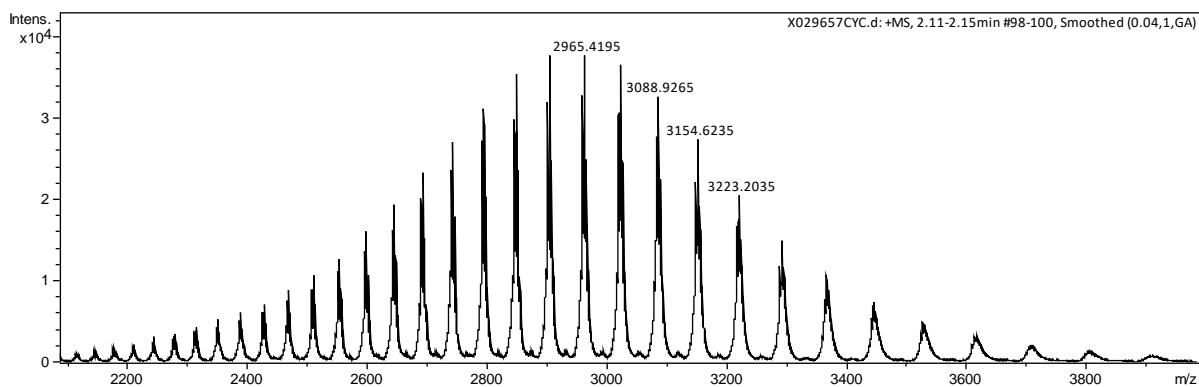
Native RTX



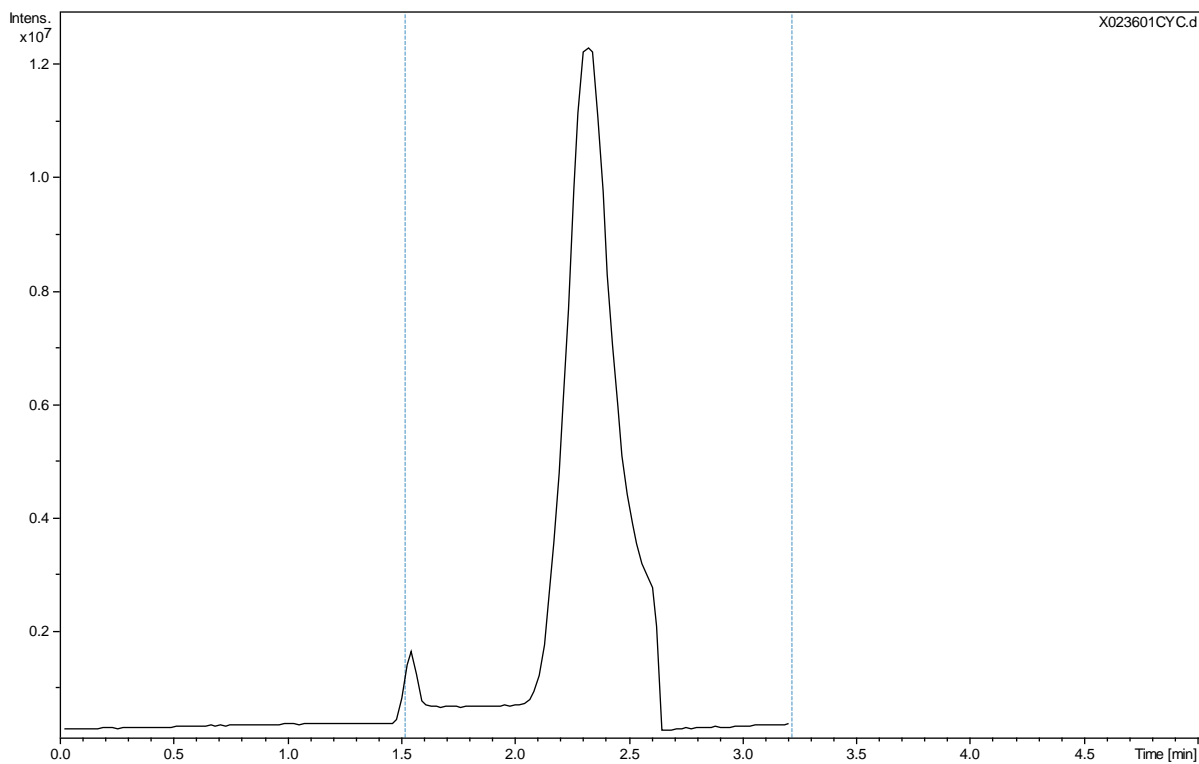
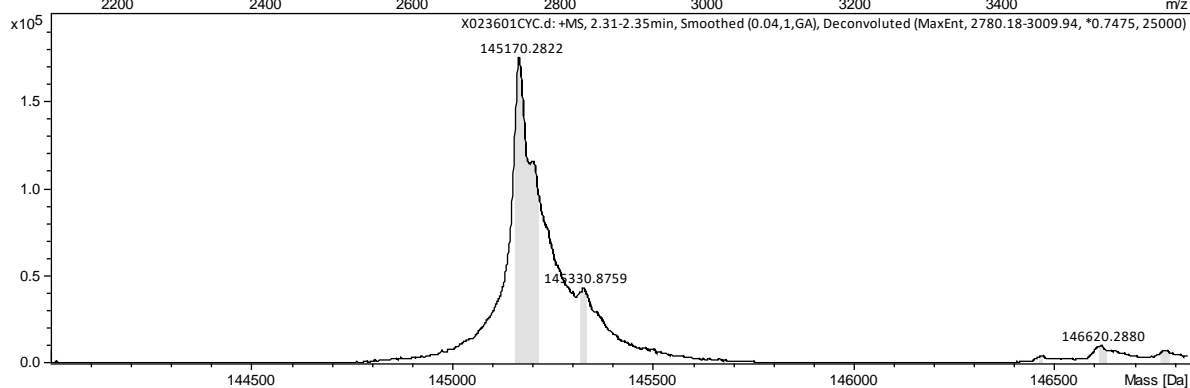
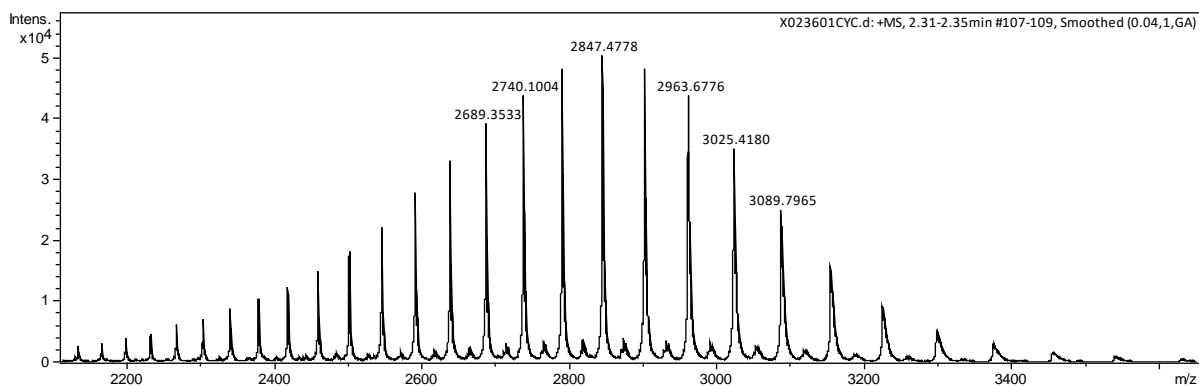
# Deglycosylated RTX



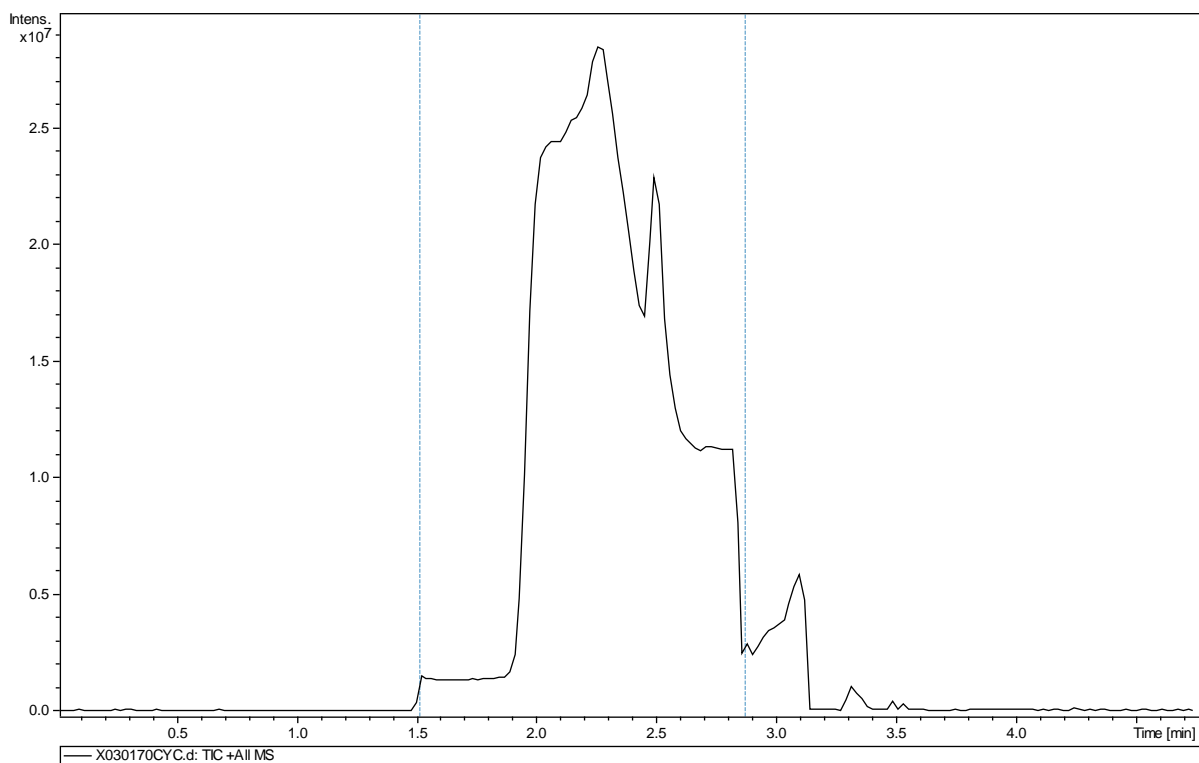
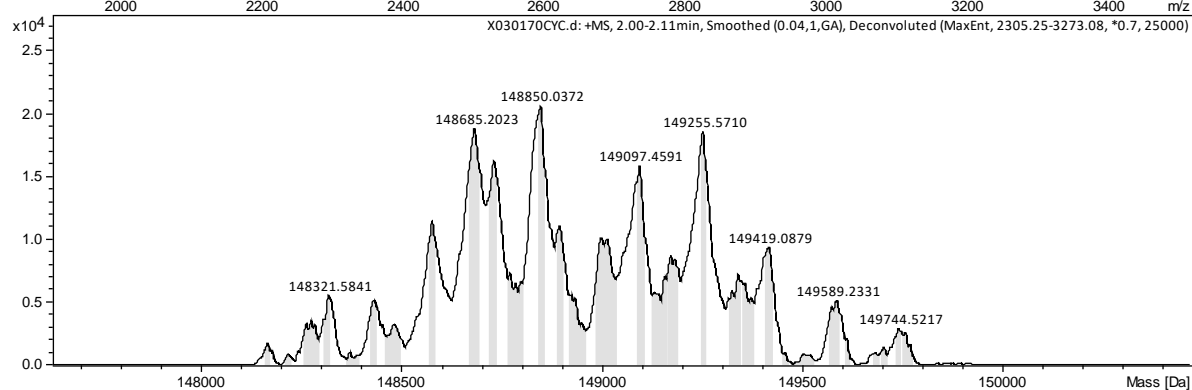
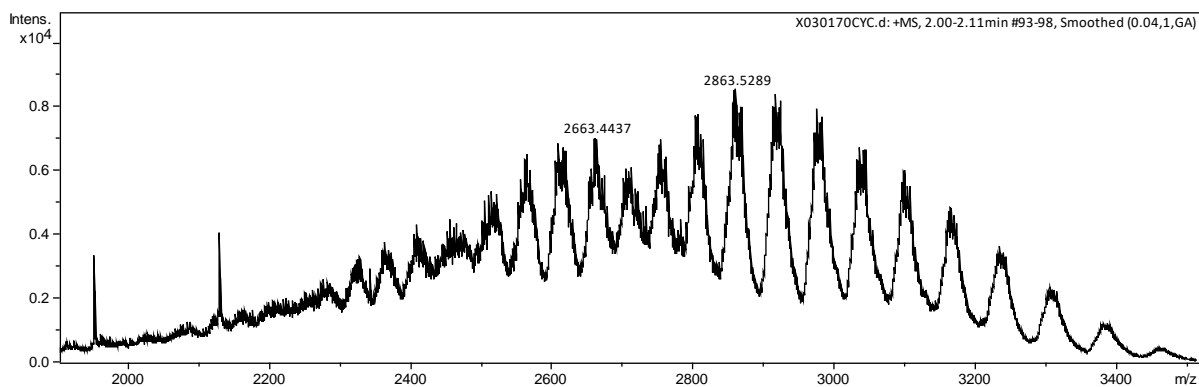
# Native TTZ



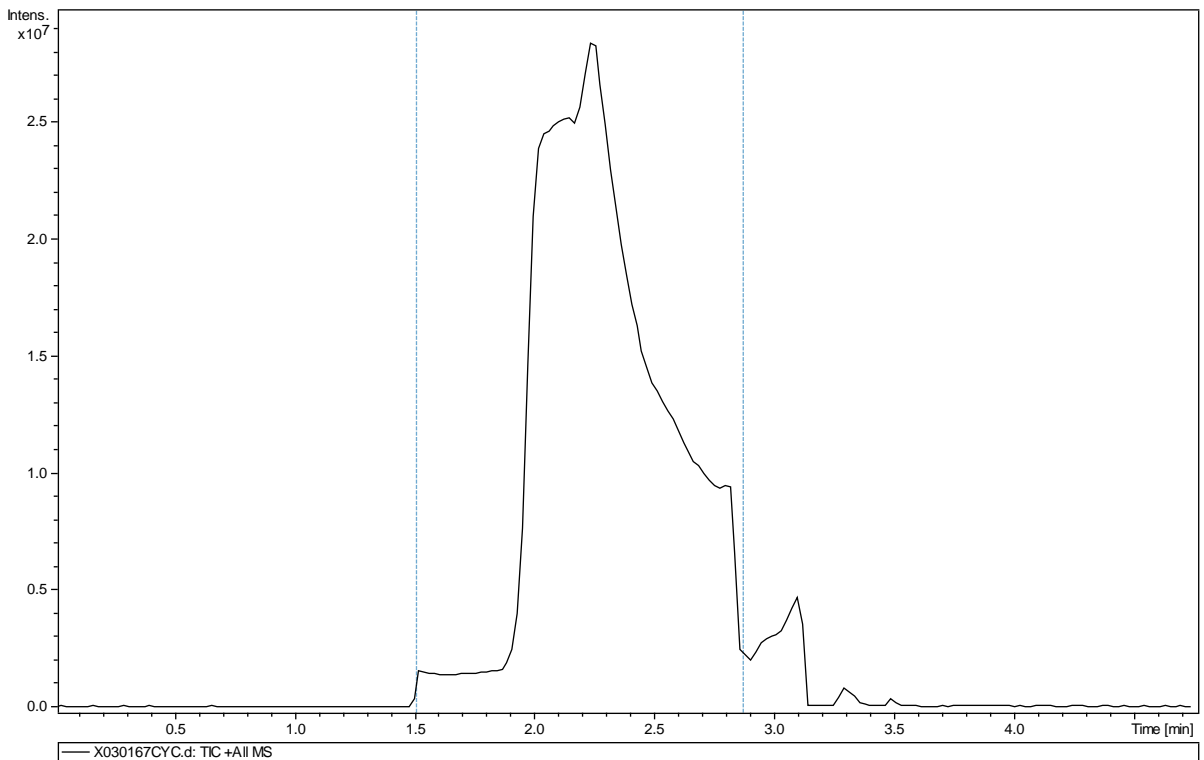
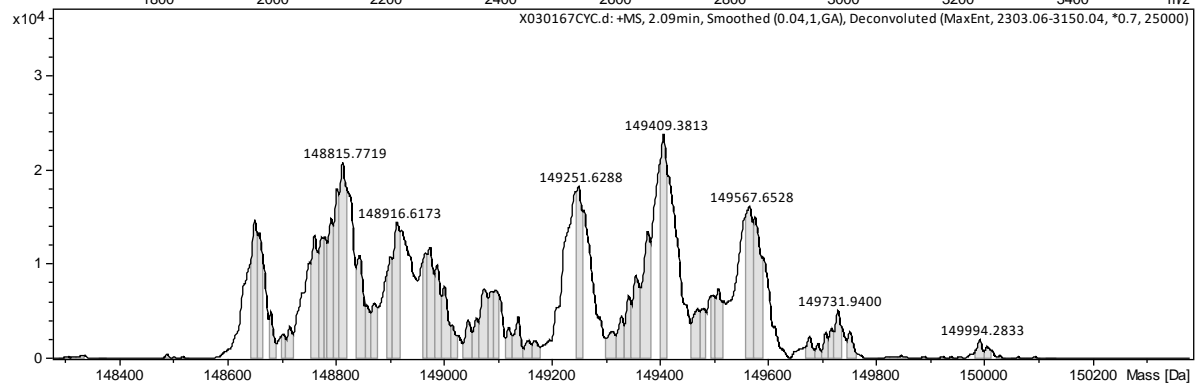
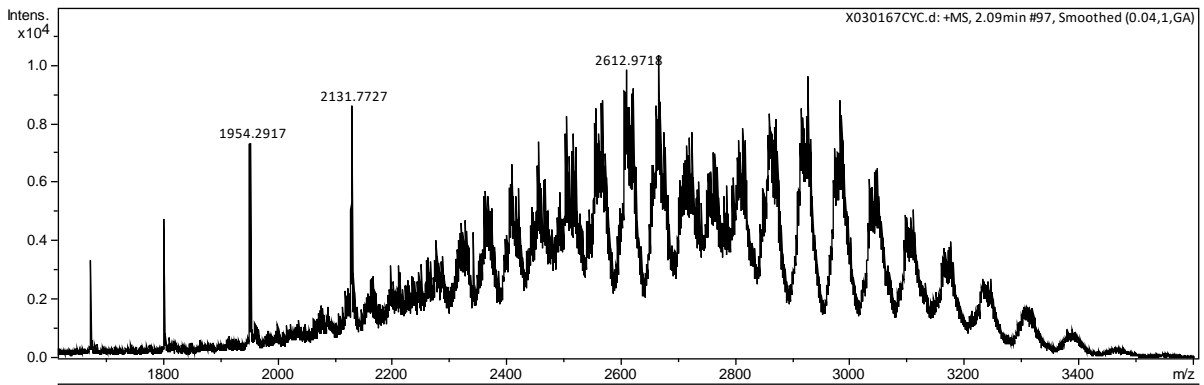
# Deglycosylated TTZ



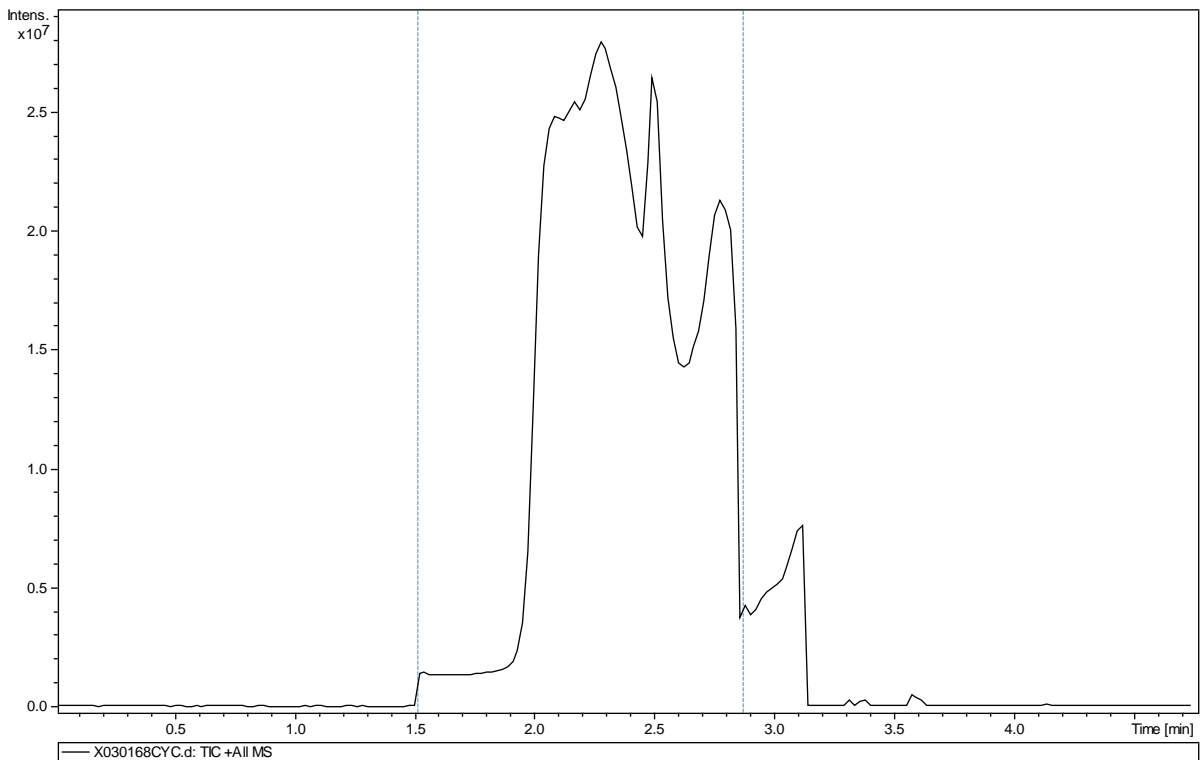
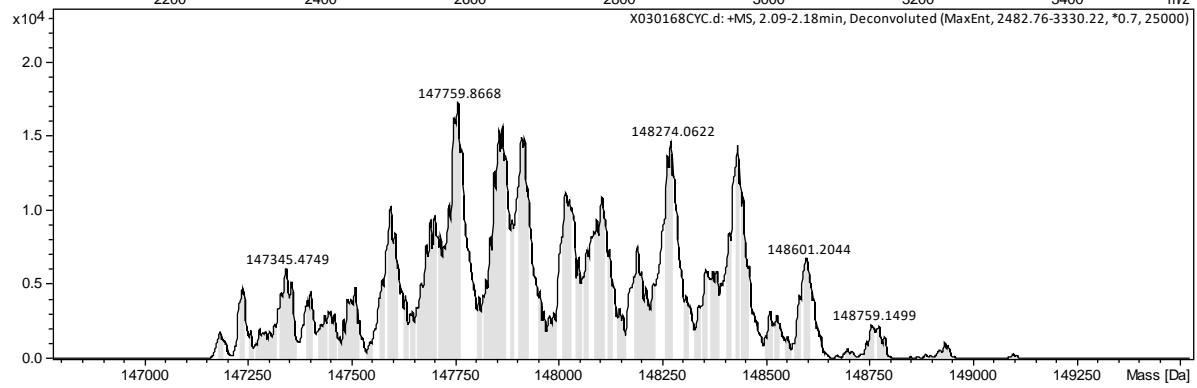
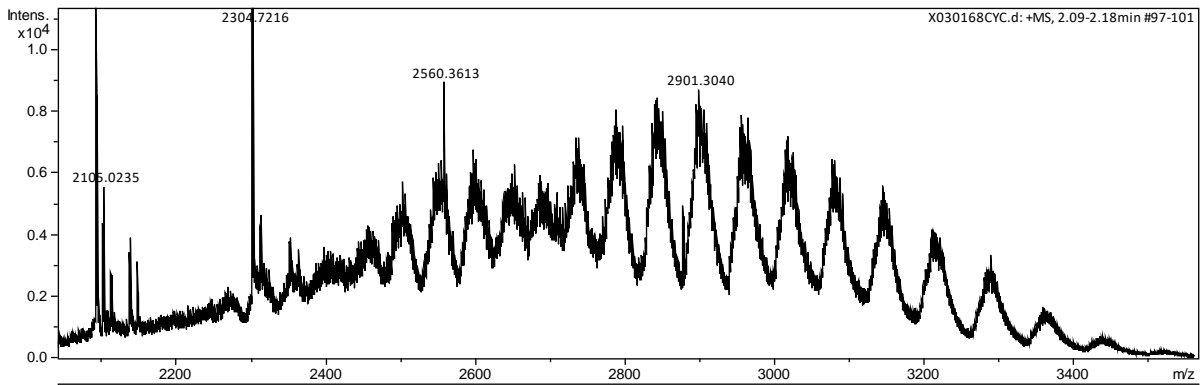
# TTZ-SGM-BDP 7a



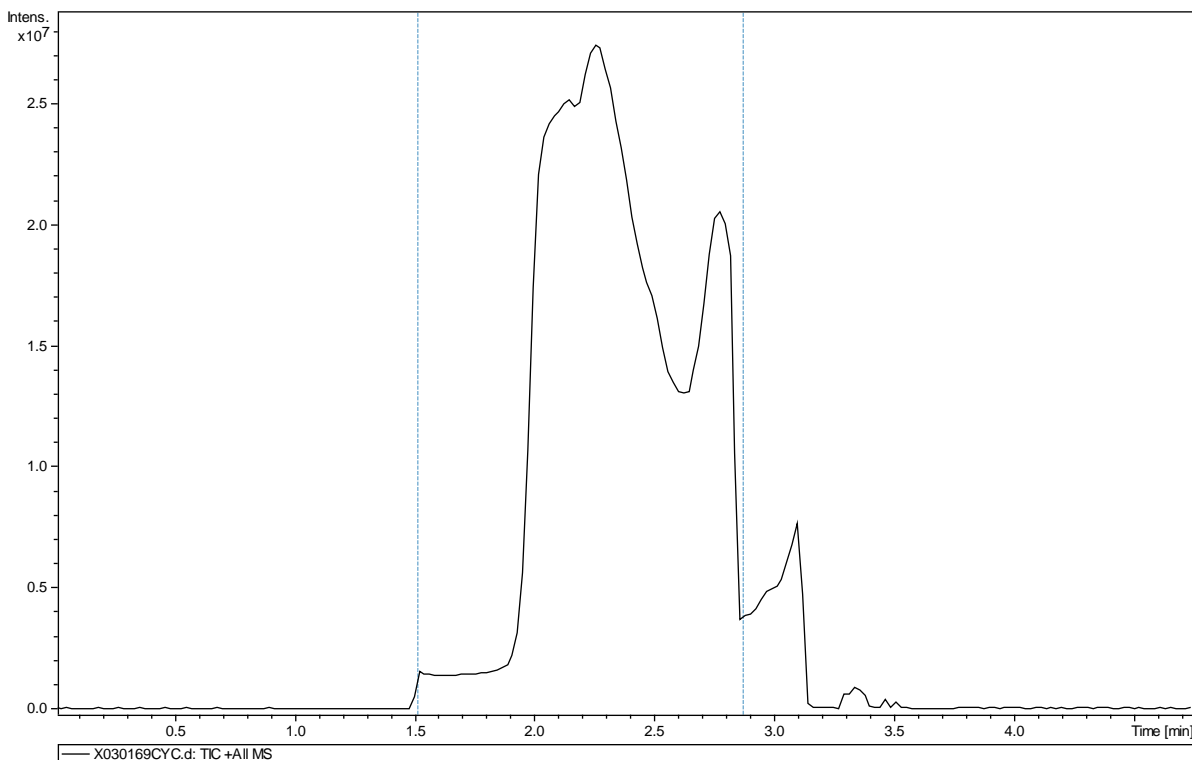
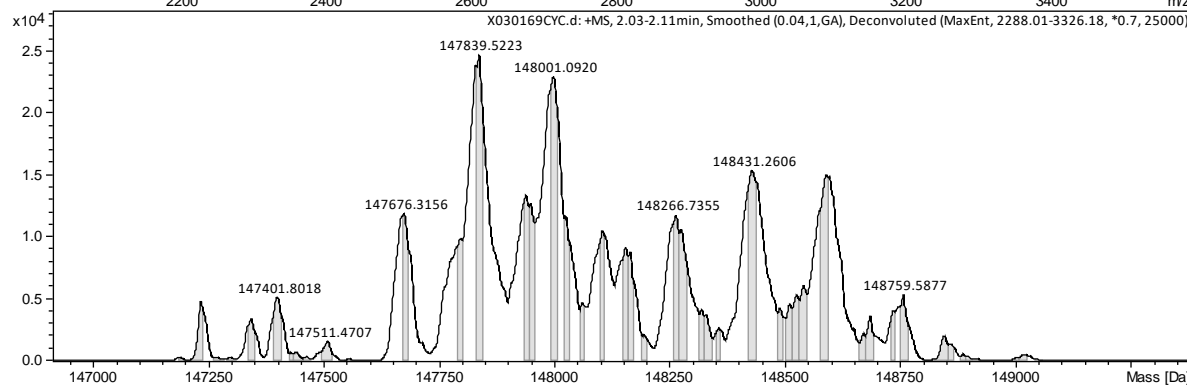
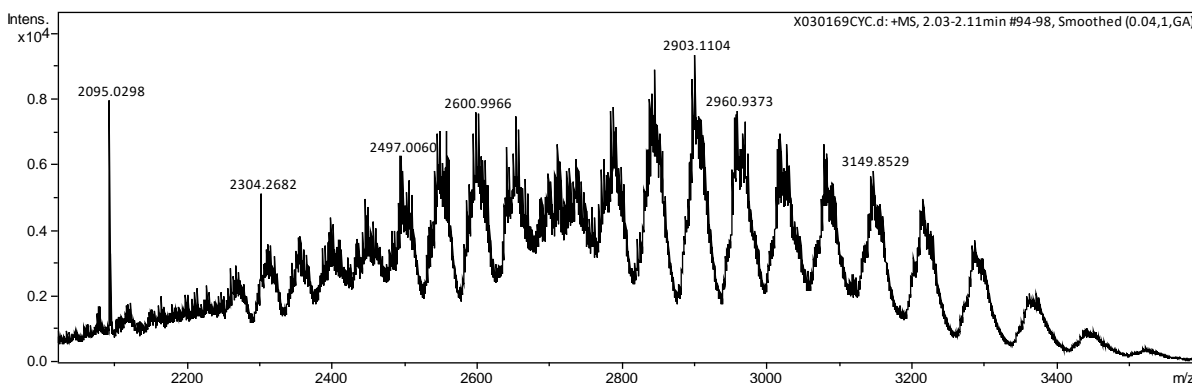
# TTZ-SGM-FLU 7b



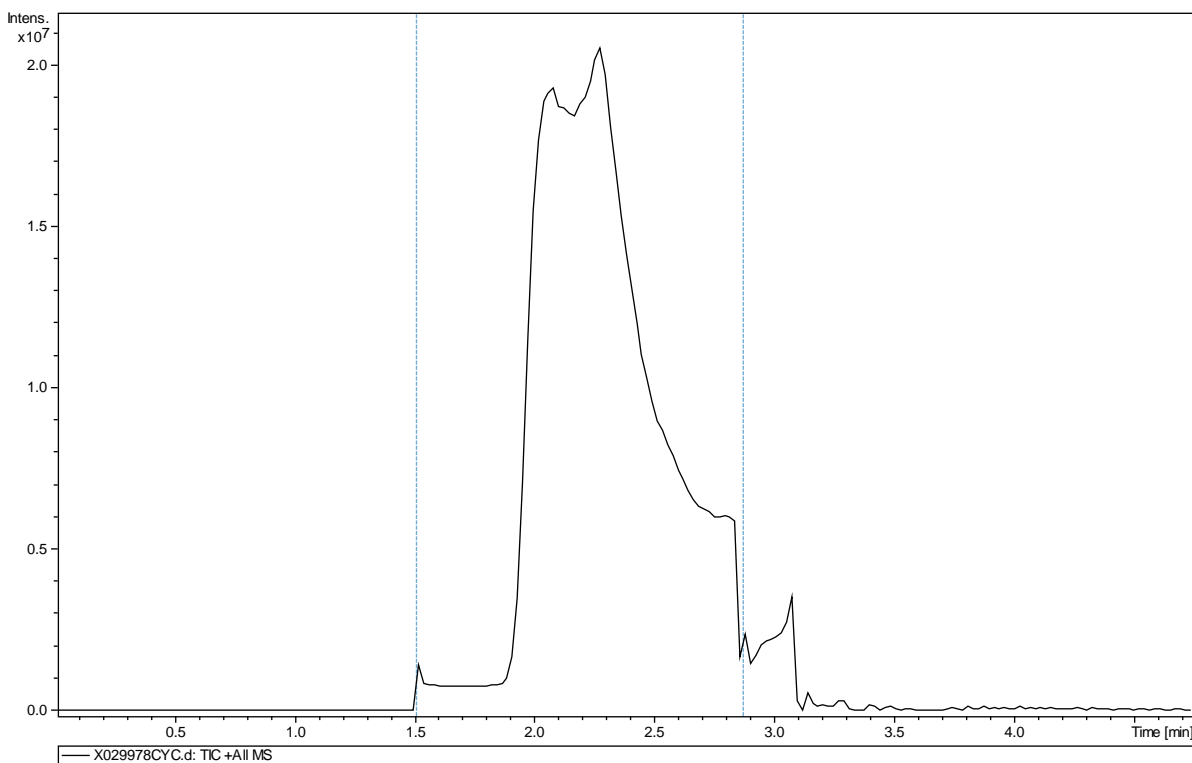
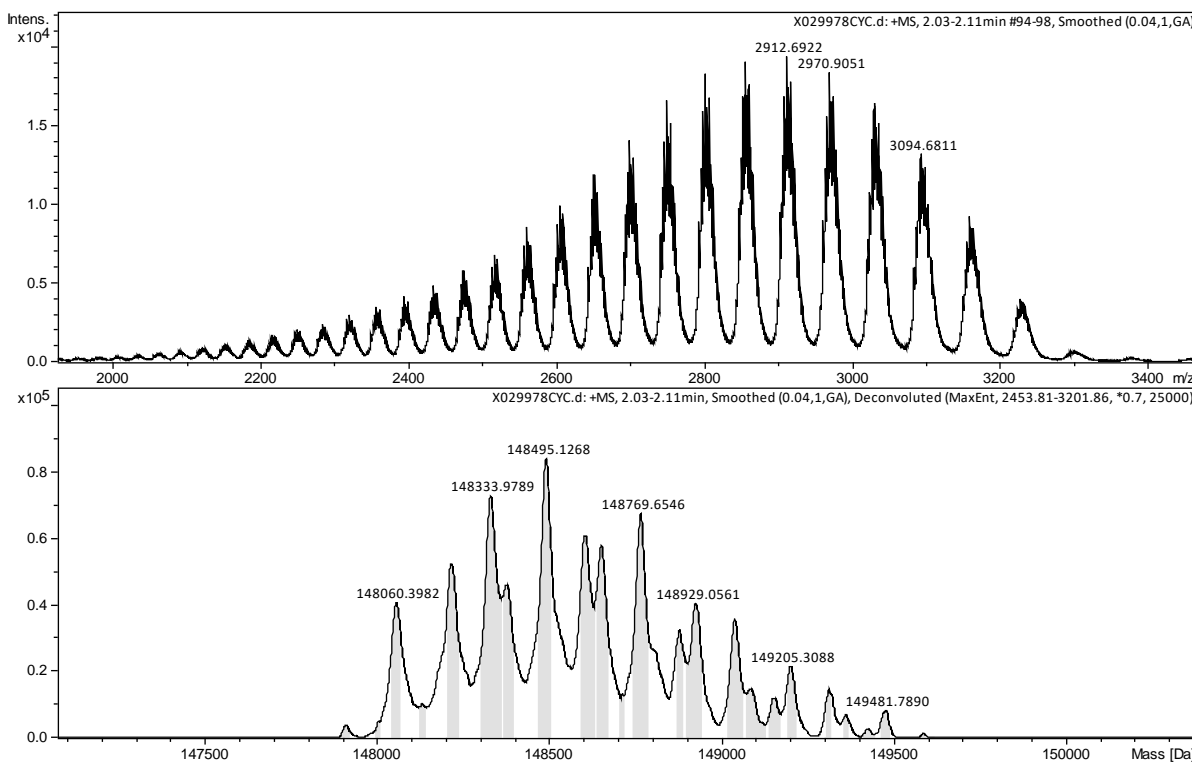
# RTX-SGM-BDP 8a



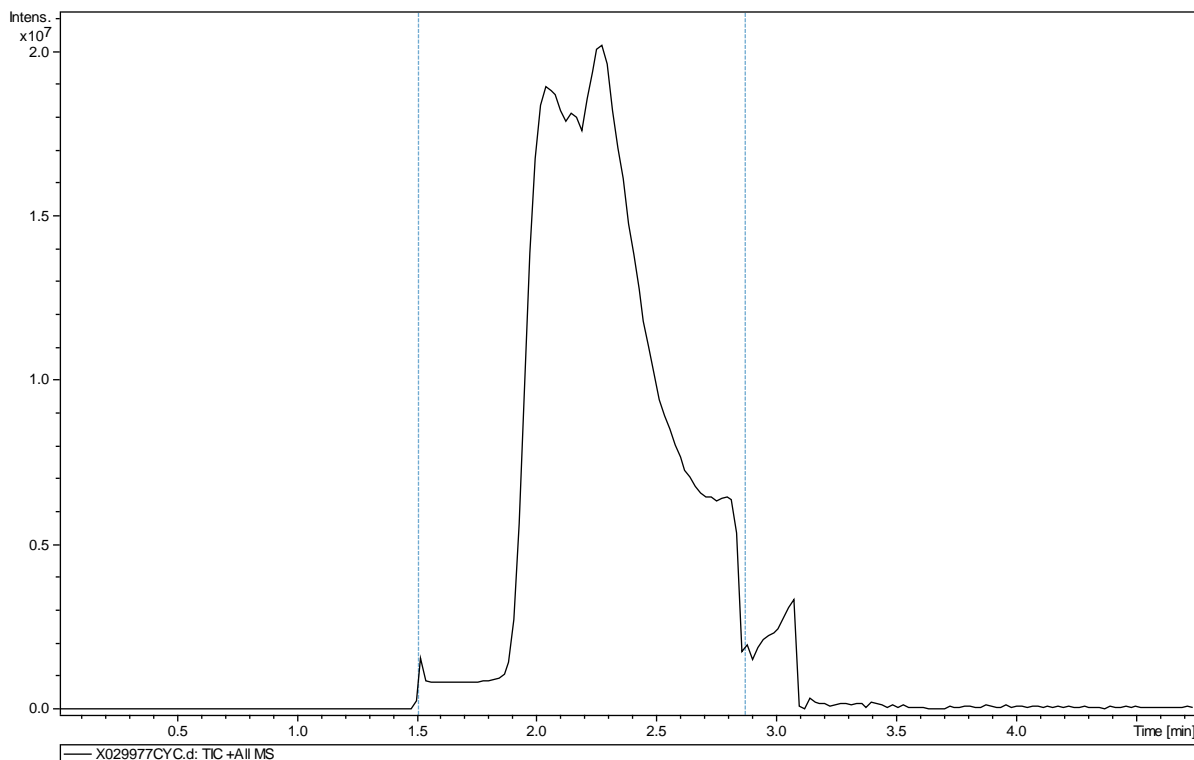
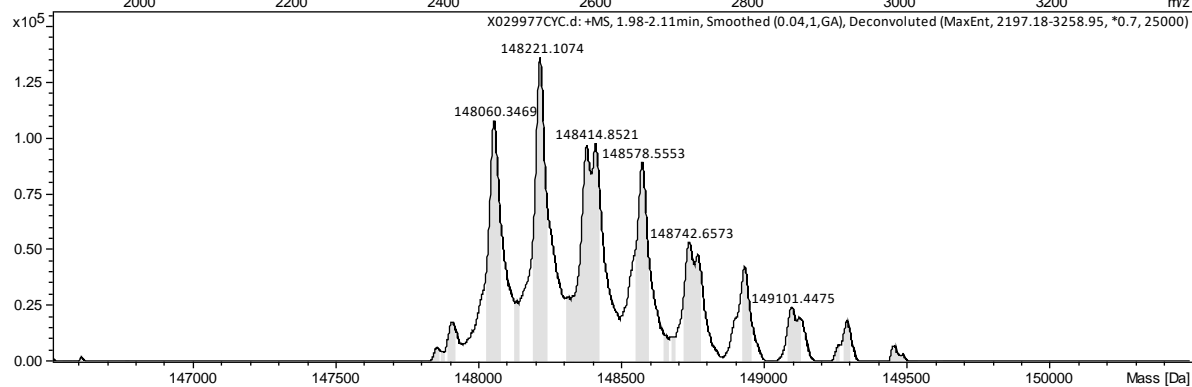
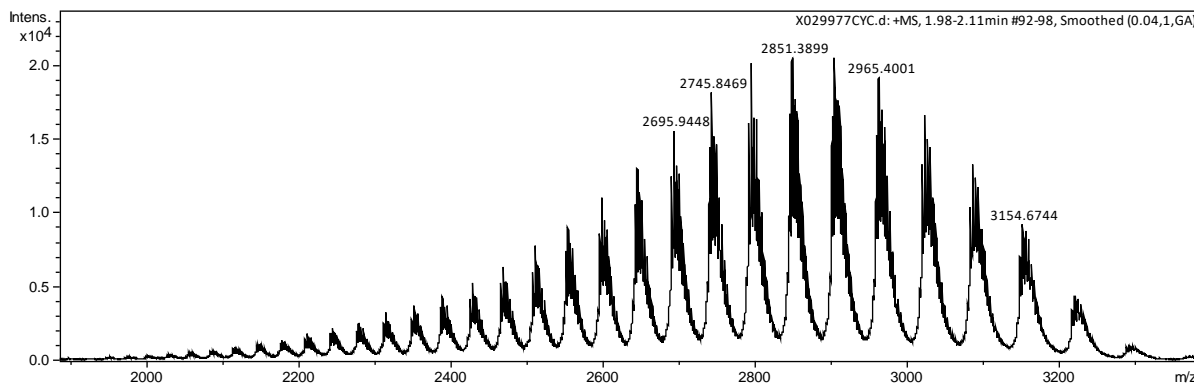
# RTX-SGM-FLU 8b



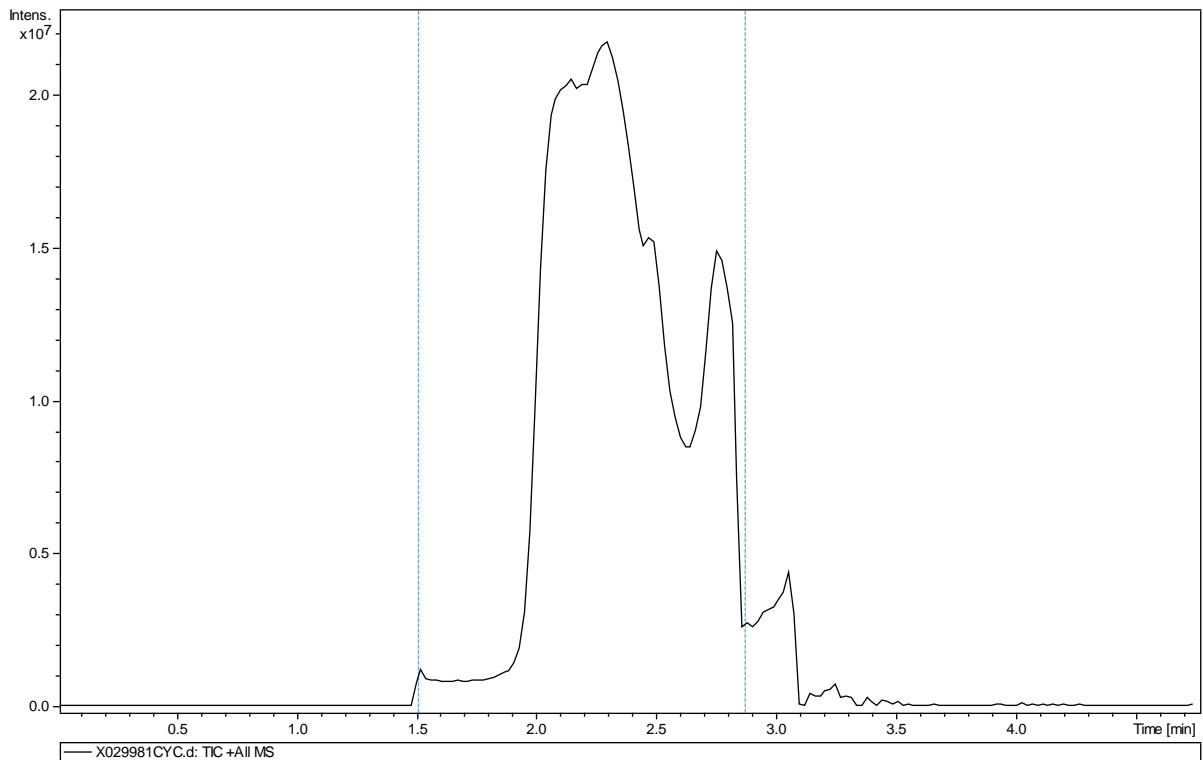
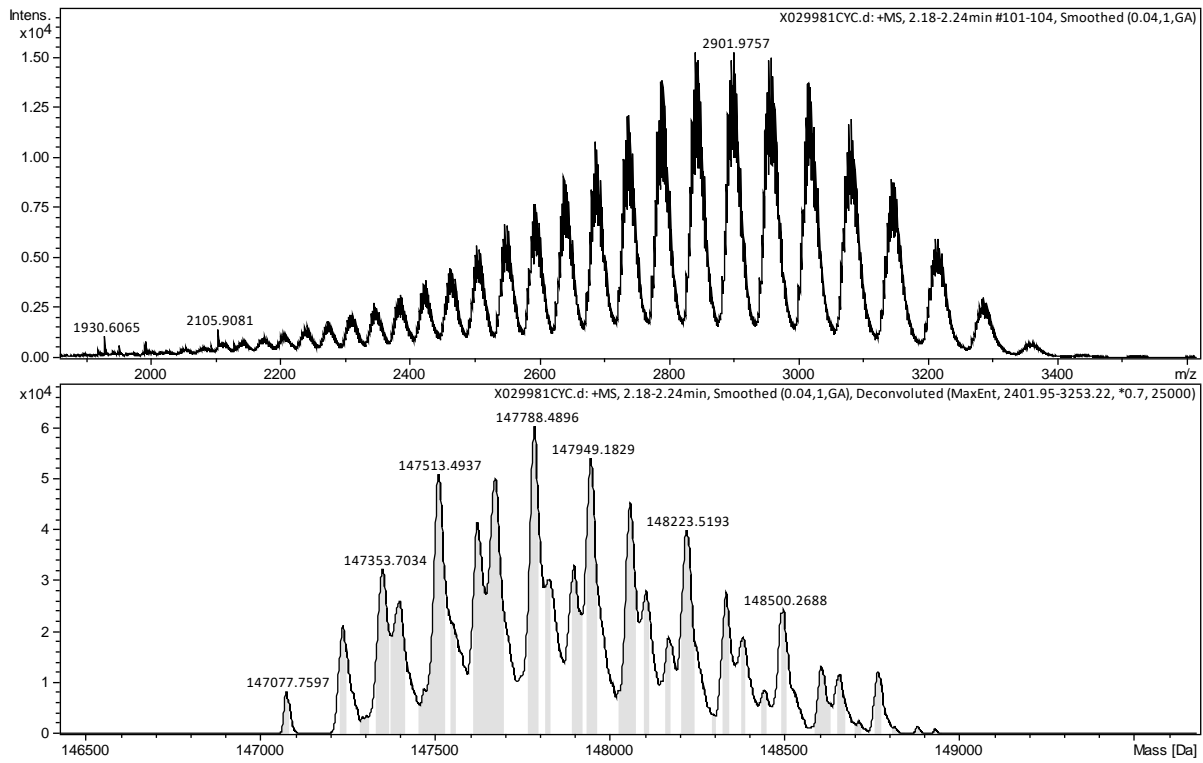
# TTZ-BDP 9a



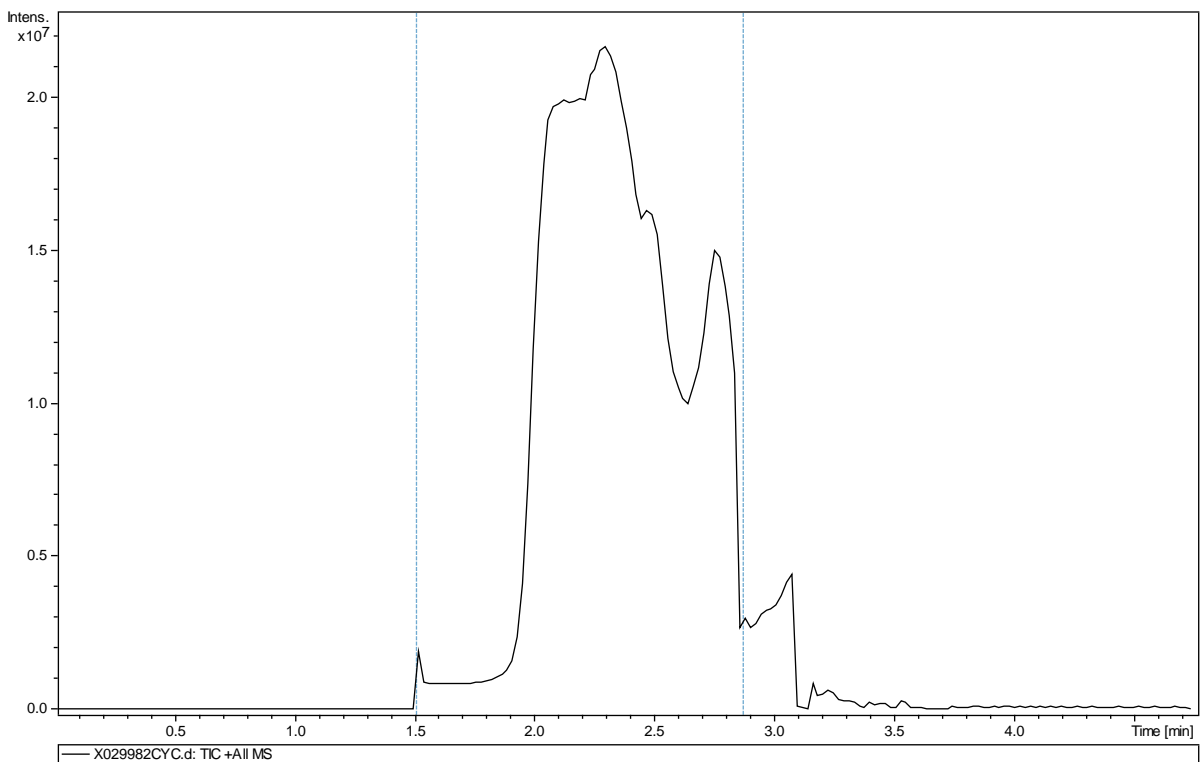
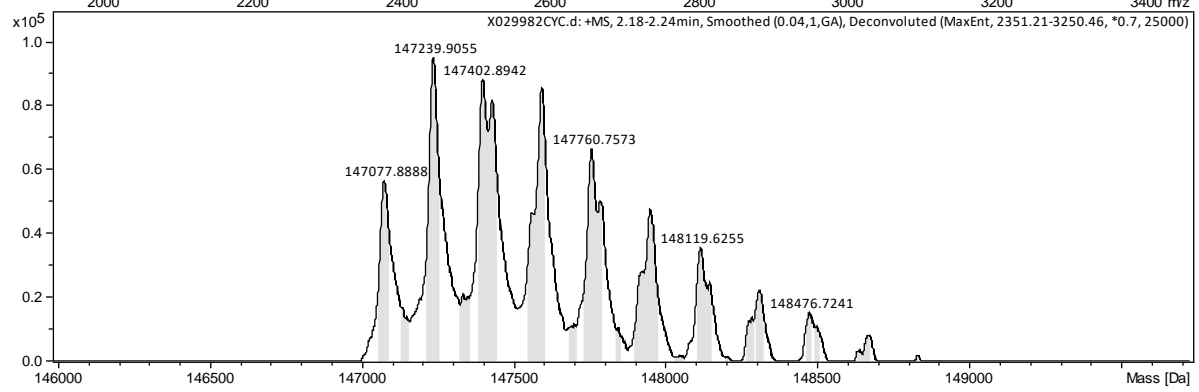
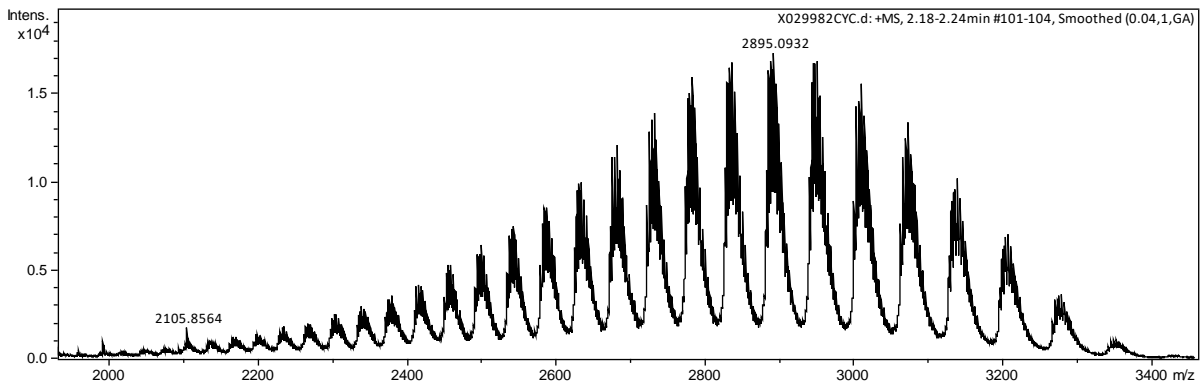
# TTZ-FLU 9b



# RTX-BDP 10a

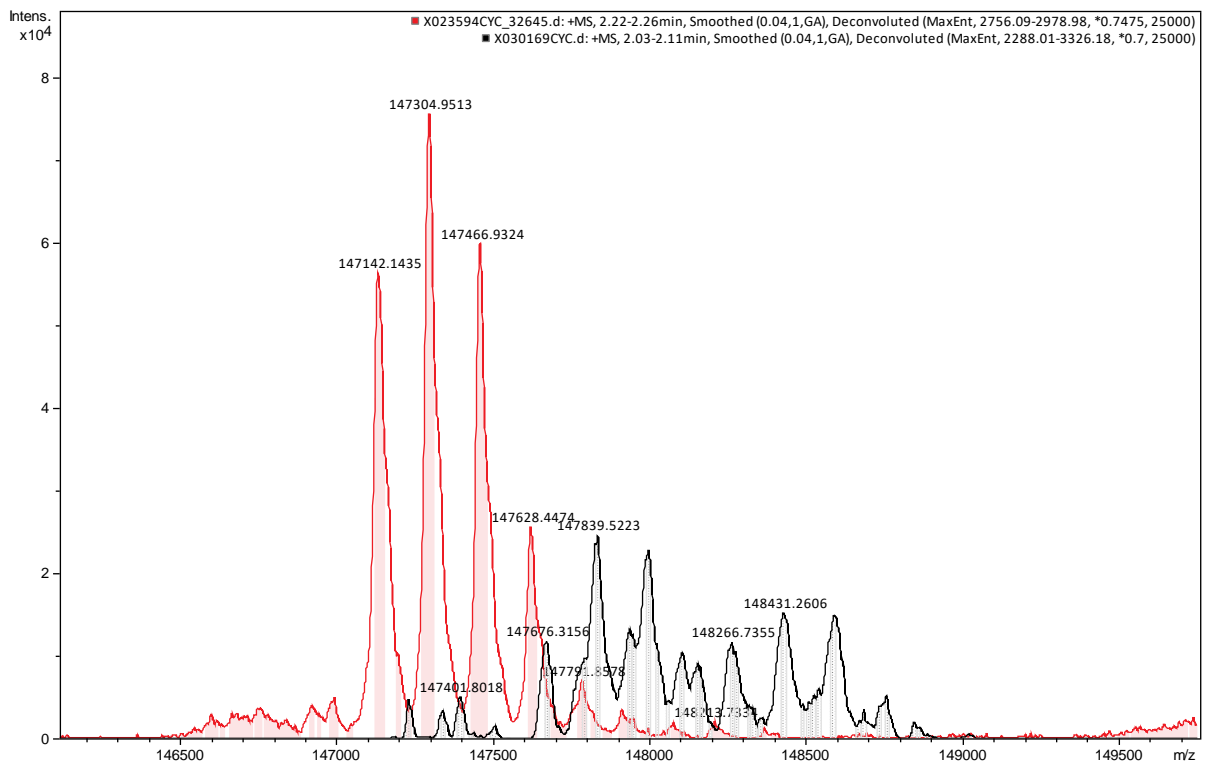


# RTX-FLU 10b



**No native mAb remains after labeling using cross-linking technology, e.g.:**

**Native RTX (red) vs RTX-SGM-FLU (black)**



To study antigen binding, we decided to focus on fluorescein-labelled AFCs **7b**, **8b**, **9b** and **10b**, considering their higher fluorescence emission and the strong quenching of BODIPY among AFCs TTZ-SGM-BDP **7a** and RTX-SGM-BDP **8a**. First, HER2 affinities of AFCs TTZ-SGM-FLU **7b** and TTZ-FLU **9b** were determined by ELISAs (**Figure S4**), between 0.01 nM and 31 nM. No difference in binding affinity between the two species was observed, with similar affinity to HER2 for AFC generated through either lysine or cross-linked conjugation.

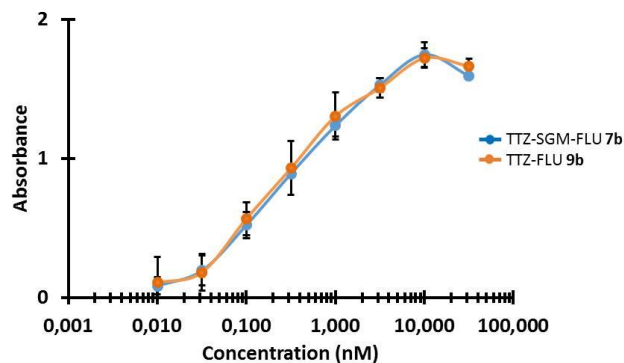


**Figure S4.** HER2 affinities of AFCs TTZ-SGM-FLU **7b** (blue curve) and TTZ-FLU **9b** (orange curve) by ELISAs.

Then, binding of AFCs RTX-SGM-FLU **8b** and RTX-FLU **10b** to CD20 were assessed using flow cytometry (**Figure S5**). Considering their fluorescence emission data (**Figure 2B**), it is possible to compare directly the binding to CD20 antigen expressed on Daudi cells *via* fluorescence ratios (**Figure S5**). Flow cytometry experiments, conducted between 1 and 100  $\mu\text{g/mL}$  of protein, showed a significant higher fluorescence ratio for AFC RTX-SGM-FLU **8b** compared to AFC RTX-FLU **10b** at pH 7 (**Figure S5**). Hence, AFC RTX-SGM-FLU **8b** had a higher binding to CD20 than AFC RTX-FLU **10b** at pH 7, which could be linked to several lysine residues very close to the CDRs of RTX (**Figure S6**). Moreover, acidification to pH 6, while reducing the fluorescence ratio of both AFCs, did not change their relative affinity to CD20 (**Figure S7**). Affinity could not be assessed in these conditions, despite important AFC concentrations. This is due to operating conditions, namely the cell concentration used for flow cytometry, which needed to be high enough for fast analysis, and the high CD20 expression at the surface of these cells, keeping us back from saturation.

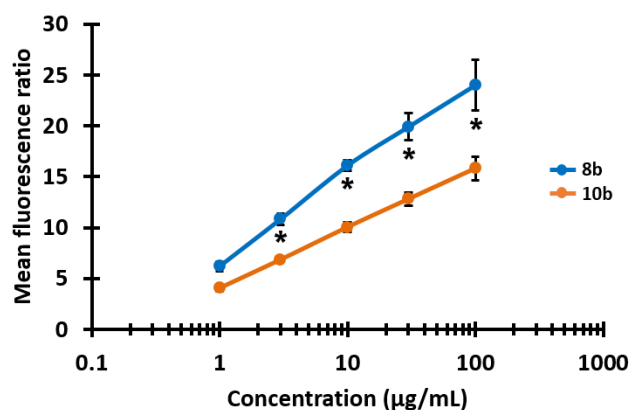


**Figure S5.** Binding of AFCs RTX-SGM-FLU **8b** (blue curve) and RTX-FLU **10b** (orange curve) to CD20 by flow cytometry.

**Table S4.** Statistical analysis on CD20 binding

		Concentration ( $\mu\text{g}/\text{mL}$ )				
		100	30	10	3	1
pH6	RTX-SGM-FLU <b>8b</b>	0.1 (n.s.)	0.4 (n.s.)	0.4 (n.s.)	0.2 (n.s.)	0.4 (n.s.)
	RTX-FLU <b>10b</b>					
pH7	RTX-SGM-FLU <b>8b</b>	0.029 (*)	0.029 (*)	0.029 (*)	0.029 (*)	0.029 (*)
	RTX-FLU <b>10b</b>					

A Wilcoxon rank sum test was used. The level of significance was set at 5% (two-sided).

p-Values of AFCs at pH 7 and pH 6 are presented.

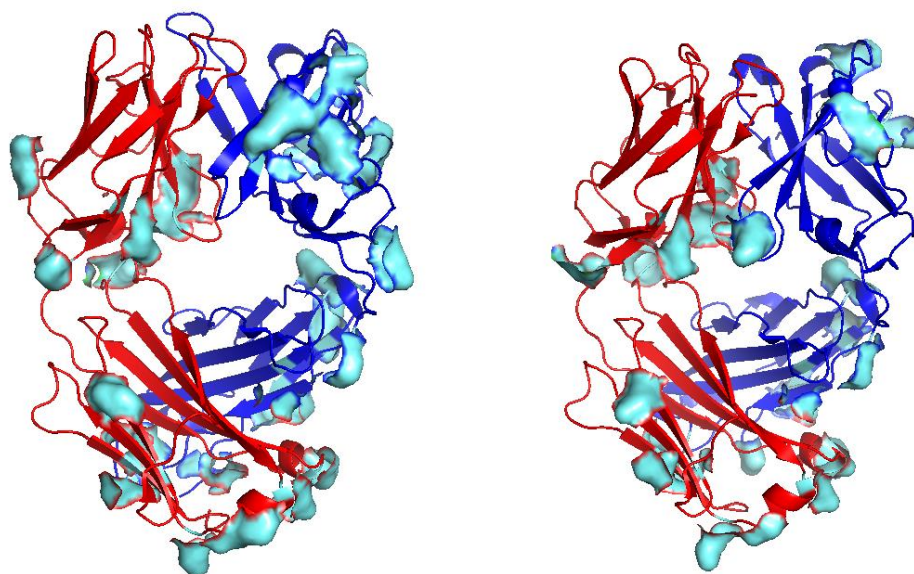


**Figure S6.** Models representing rituximab (left) and trastuzumab (right), from PDB structures 2OSL and 4HKZ respectively. Heavy (blue) and light (red) chains are represented as cartoons, and lysines are visualized as cyan surfaces. In the V-domains, trastuzumab contains 9 lysine residues (4 in VH and 5 in VL), among which one is contained inside CDRH1 and 2 others in the heavy chain framework are close to the paratope. For rituximab, the V-domains include 12 lysine residues among which 6, all inside the heavy chain, are very close to the paratope.

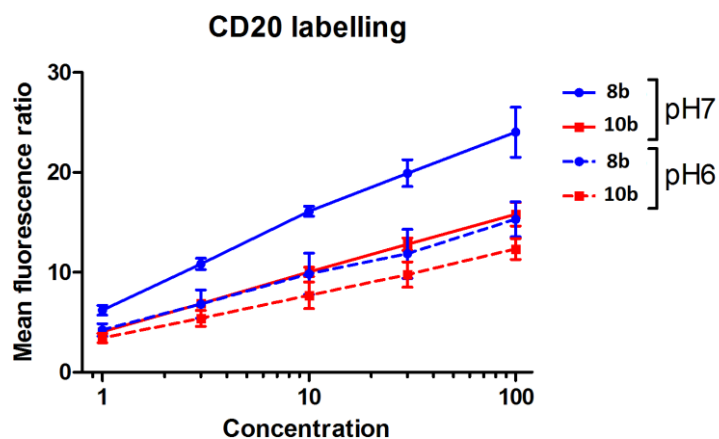


**Figure S7.** Flow cytometry of AFCs RTX-SGM-FLU **8b** and RTX-FLU **10b** at pH7 and pH6, n = 3

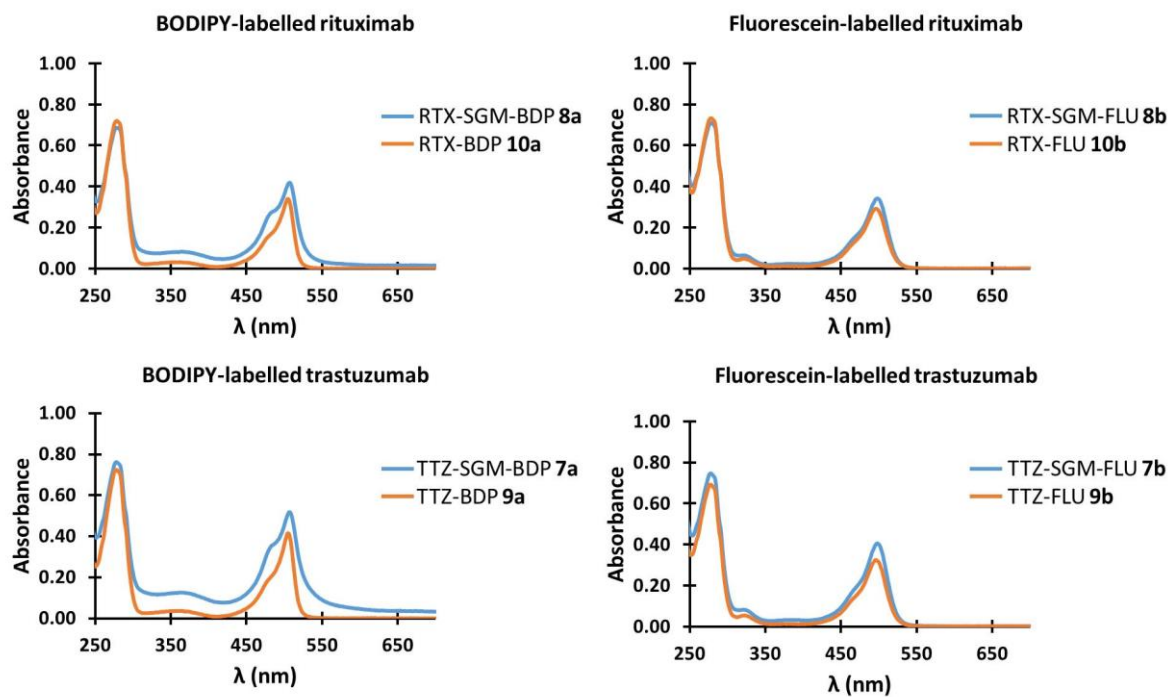


**Figure S8.** UV-visible absorption of AFCs. Sample concentration was adjusted to 500  $\mu\text{g/mL}$  of protein.

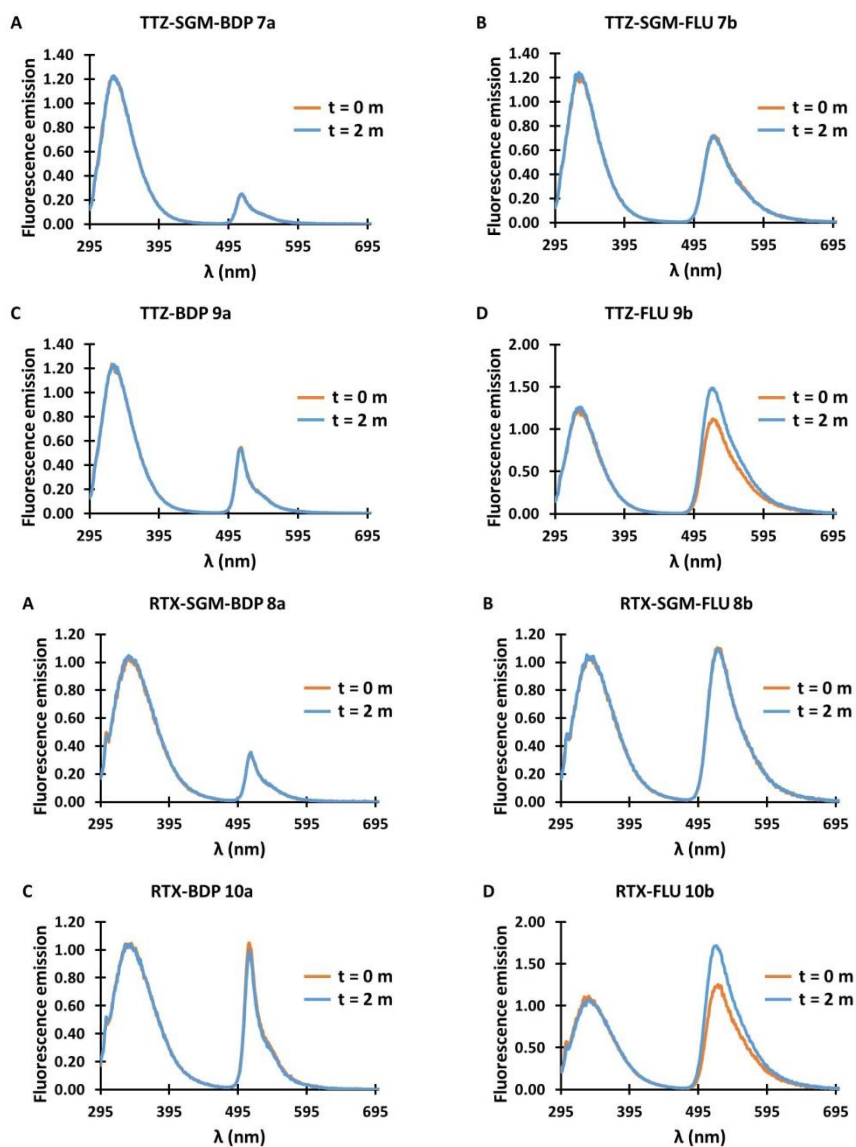


**Figure S9.** Fluorescence emission of fresh (orange curves) and stored in the dark at 4 °C (blue curves) AFCs based on rituximab after normalisation. Excitation wavelength: 275 nm. For easier comparison, the sample concentration was adjusted to 50  $\mu\text{g}/\text{mL}$  of protein.

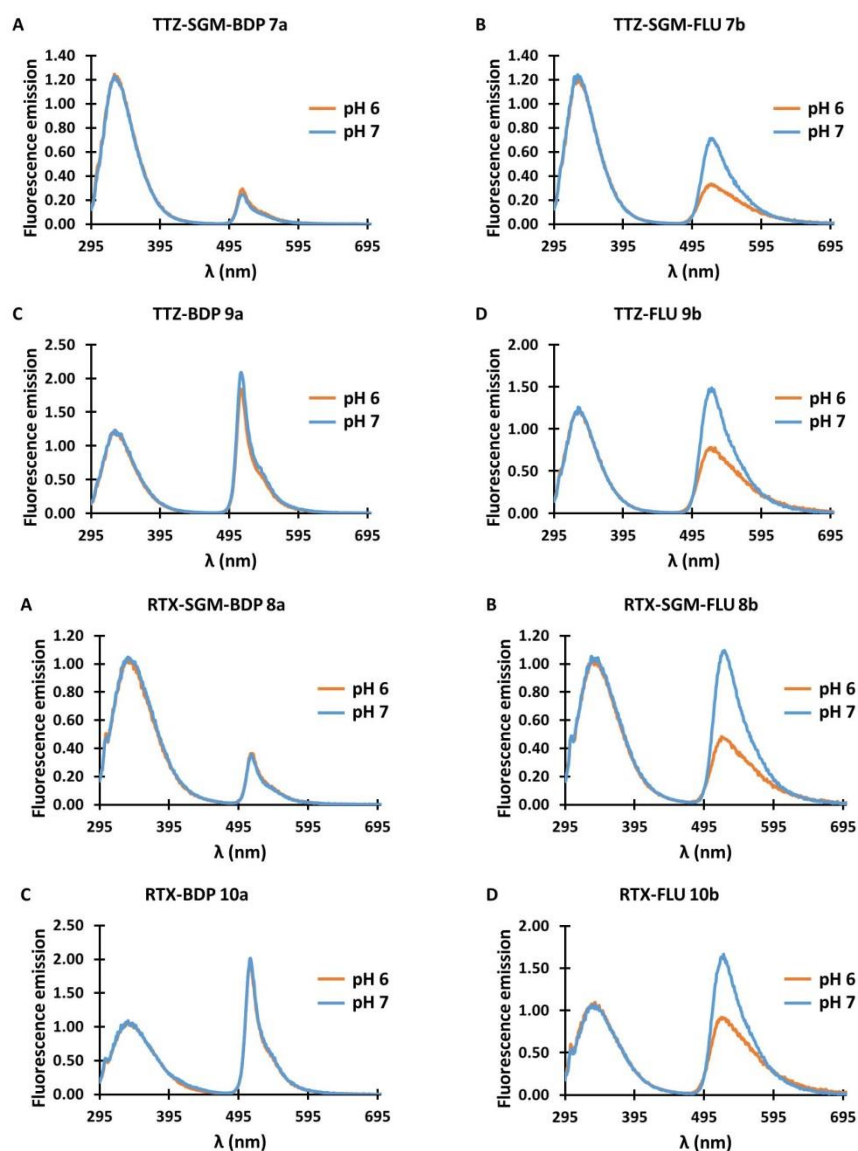


**Figure S10.** Comparison of fluorescence emission of AFCs based on rituximab at pH 7 (blue curves) and 6 (orange curves) after normalisation. Excitation wavelength: 275 nm. For easier comparison, the sample concentration was adjusted to 50  $\mu\text{g/mL}$  of protein.

## References

- (1) Castañeda, L., Wright, Z. V. F., Marculescu, C., Tran, T. M., Chudasama, V., Maruani, A., Hull, E. A., Nunes, J. P. M., Fitzmaurice, R. J., Smith, M. E. B., Jones, L. H., Caddick, S., and Baker, J. R. (2013) A mild synthesis of N-functionalised bromomaleimides, thiomaleimides and bromopyridazinediones. *Tetrahedron Lett.* 54, 3493–3495.
- (2) Suzuki, T., Hisakawa, S., Itoh, Y., Suzuki, N., Takahashi, K., Kawahata, M., Yamaguchi, K., Nakagawa, H., and Miyata, N. (2007) Design, synthesis, and biological activity of folate receptor-targeted prodrugs of thiolate histone deacetylase inhibitors. *Bioorganic Med. Chem. Lett.* 17, 4208–4212.